FACULTY OF SCIENCES

Investigation of biologically induced Pt isotope fractionation in response to Pt-based chemotherapeutic drug resistance

Milan Felix

Promotor: Prof. Dr. Frank Vanhaecke
Co-promoter: Dr. Kaj Sullivan

A dissertation submitted to Ghent University in partial fulfilment of the requirements for the degree of Master of Science in Chemistry

Academic year 2023-2024

GHENT UNIVERSITY

Page left intentionally blank.

FACULTY OF SCIENCES

MASTER THESIS

INVESTIGATION OF BIOLOGICALLY INDUCED PT ISOTOPE FRACTIONATION IN RESPONSE TO PT-BASED CHEMOTHERAPEUTIC DRUG RESISTANCE

Milan Felix
Student number: 01900180

(co-)promotors: Prof. Dr. Frank Vanhaecke, Dr. Kaj Sullivan

A dissertation submitted to Ghent University in partial fulfilment of the requirements for the degree of Master of Science in Chemistry

Academic year: 2023 – 2024

GHENT UNIVERSITY

Page left intentionally blank.

Preface and acknowledgments

This thesis consists out of two separate parts. The first part is referred to as the research plan and the second part is known as the research project. Preliminary research and a literature study were conducted during the research plan phase, which started February 2023 and ended May 2023. Most of the experiments were carried out during the research project phase, which lasted from September 2023 until January 2024, with experimental work ending in December 2023. The two parts combined form the full master thesis. This preface serves as a short overview to clarify what can be expected from the thesis.

Ahead of the thesis is a summary in the form of a publication. The general outline, most important data and a conclusion can be found here. Following this summary is the research plan, unaltered compared to the version that was submitted in May 2023, excluding the references. These references can be found with more recent ones at the end of the full thesis. Next is the main part of the thesis, the research project. Here the experiments are described and results of these experiments are discussed.

Firstly, I would like to thank my supervisor Dr. Kaj Sullivan for his valuable guidance during the experimental work of this thesis and his active involvement in the writing part as well. He also assisted me every time I needed help processing the experimental data or whenever I could not finish my experiments due to overlap with courses. Secondly, I would like to thank my promotor Prof. Dr. Frank Vanhaecke and the A&MS research group for welcoming me in the group and allowing me to carry out my thesis here. I am especially grateful for Floor and Nico, two of my favorite people in the world, who supported and aided me during every step of this thesis to make sure I never gave up. The same can be said for Luna, Sien and Stef, who were my classmates and best friends over the course of my 5 years at university. Finally I would like to thank my mom, dad, two brothers and all my family members and friends whose name I did not mention that assisted me in any way in finishing this thesis, by either proofreading, helping with technical difficulties or supporting me in general. I could not have written this thesis without all this help.

Page left intentionally blank.

Investigation of Biologically-Induced Pt Isotope Fractionation in Response to Pt-based Chemotherapeutic Drug Resistance.

M. Felix[a], K. V. Sullivan[a], and F. Vanhaecke[a]

[a] A&MS Research Group, Department of Chemistry, Ghent University, Krijgslaan 281-S12, Ghent, Belgium

The goal of this research was to determine whether resistance of ovarian cancer cells to cisplatin is reflected in changes in Pt isotope fractionation. Both cisplatin-sensitive (A2780) and cisplatin-resistant (A2780cis) ovarian cancer cells were treated with cisplatin, with the aim of measuring Pt isotope ratios in these samples after treatment. A chromatographic procedure to separate Pt from the matrix elements is reported. Synthetic samples were measured using MC-ICP-MS to assess the accuracy and precision attainable in Pt isotopic analysis. The influence of contaminating elements and a concentration mismatch between samples and bracketing standard on Pt isotopic analysis was also determined. On-column fractionation of Pt was investigated and fractions eluted from the column were measured for possible contamination originating from the column. Ultimately, the Pt isotope ratios in the cell samples were not determined but this research lays the foundation for future ovarian cancer research using Pt isotopic analysis.

Key words: Pt isotope fractionation, chromatographic Pt isolation, MC-ICP-MS, ovarian cancer, cisplatin

---

Introduction

Isotopes of an element are atoms with the same number of protons, but a different number of neutrons in the nucleus. That is, they have the same atomic number, but a different mass number and therefore a different mass (1). The term "isotope fractionation" refers to the relative partitioning of "heavy" (higher mass) and "light" (lower mass) isotopes between two co-existing phases in a system (2). Isotopes will redistribute as a function of their mass, a property which is used in the field of *biomedical isotopic analysis*, where variations in bodily stable metal isotope ratios are studied in the context of biomedicine (2). The emergence of this field is due to the development of the MC-ICP-MS technique, which allows high-throughput and high-precision isotopic analysis owing to the simultaneous measurement at multiple mass-to-charge ratios (3).

Metal dysregulation is often inherent to cancers and other diseases and can result in systemic changes to essential mineral element (Mg, K, Ca, Fe, Cu and Zn) stable isotopic compositions (4). Chemotherapy using Pt-based compounds (e.g. cisplatin) is a standard treatment, but tumors that are initially responsive may develop chemoresistance, resulting in treatment failure (5). Several mechanisms underlying tumor cell resistance have been

identified so far, including the altered expression of ion channels (Na, Mg, K, and Ca) and Fe-, Cu-, and Zn-binding proteins, but these remain poorly understood and it is unclear whether they can be exploited as markers of resistance (6-8). However, there is a significant correlation between high-affinity Cu uptake protein 1 (CTR1) expression and cisplatin accumulation in the A2780 and A2780cis ovarian cancer cell lines, demonstrating a link between Cu homeostasis and cisplatin uptake (9). Altered Cu homeostasis has also been demonstrated in four strains of cisplatin-resistant yeast, with the decreased expression of CTR1 being associated with increased $^{65}Cu/^{63}Cu$ values, demonstrating the potential of isotopic analysis as a marker of chemoresistance (10).

Although Pt isotopic analysis finds application in aiding to constrain terrestrial core formation and other geochemical processes, it is yet to be applied in a biomedical context (11-13). However, it is common for cancers, such as ovarian cancer, to develop resistance during the prolonged treatment process, and a strong case can be made for investigating whether the Pt isotopic composition of the drug (cisplatin) reaching the affected cells is altered when its normal functioning is disrupted.

Firstly, to accurately determine the Pt isotopic composition, a chromatographic procedure to separate Pt from all other elements that could be present in a biological matrix is needed. This procedure was developed starting from existing methods, but these methods were developed for geological samples (11,13). The first step in this research was therefore to simplify these procedures, since a biological matrix is much less complex compared to these geological matrices.

This research also comprised development of a method to determine the Pt isotopic composition of samples using a Neptune *Plus* MC-ICP-MS unit (ThermoScientific, Bremen, Germany). The accuracy and precision of this method could be tested by comparing the results to those of previous research (13). The results can be compared because the same standard reference material and Pt standard was used as those used by Poole et al.

Experimental

Materials and reagents

To minimize the potential of contamination, all sample preparation procedures were performed in a class-10 clean room laboratory (PicoTrace, Göttingen, Germany). Ultra-pure water was prepared using a Milli-Q water purification system (Merck Millipore, Molsheim, France). Pro-analysis grade HNO_3 (Chem-Lab, Zedelgem, Belgium) and HCl (Fisher Chemicals, Loughborough, UK) were further purified by subboiling distillation in a Savillex DST-4000 acid purification system (Savillex Corporation, Eden Prairie, MN, USA). Whenever concentrations had to be determined, Ga (Inorganic Ventures, VA, USA) was added as an internal standard. Hydrogen peroxide (H_2O_2) was also used for post-column sample treatment and sample digestion.

The variations in Pt isotope ratios are reported in terms of deviation of an isotope ratio for a sample compared to the same isotope ratio in a standard. Since these shifts in isotope ratios are typically very small they are reported as δ-values. δ-values are always calculated relative to a standard or reference material. The isotopic reference material used in this research was the IRMM-010 certified reference material. Platinum-α (Pt-α) was used as an in-house Pt standard to prepare synthetic Pt samples with a known δ-value (-0.07 ± 0.03 ‰) relative to IRMM-010 (13).

(MC-)ICP-MS instruments

Isotope ratio measurements were performed using a Neptune *Plus* MC-ICP-MS unit (ThermoScientific, Bremen, Germany). The advantage of using this instrumentation is that it is equipped with 10^{13} Ω Faraday cup resistors, which improves the ability to perform precise Pt isotope ratio measurements at low Pt concentration (14). The instrument settings can be found in Table I.

TABLE I. Neptune MC-ICP-MS operating conditions.

Instrument settings	
Forward power	1200 W
Plasma gas flow rate	15.0 L Ar min^{-1}
Auxiliary gas flow rate	0.70 to 0.95 L Ar min^{-1}
Nebulizer gas flow rate	~1 L Ar min^{-1}
Sample cone	Nickel, Jet-type: 1.1 mm orifice diameter
Skimmer cone	Nickel, X-type: 0.8 mm orifice diameter
Sample uptake rate	0.1 mL min^{-1}
Mass resolution mode	Low
Data acquisition parameters	
Faraday cup configuration / amplifier	L3 (^{191}Ir)/10^{11} Ω, L1 (^{193}Ir)/10^{11} Ω, C (^{194}Pt)/10^{13} Ω, H1 (^{195}Pt)/10^{13} Ω, H2 (^{196}Pt)/10^{13} Ω, H3 (^{198}Pt)/10^{13} Ω
Sensitivity	0.33 V for ^{195}Pt at 10 ng mL^{-1} (ppb)
Signal integration time	4 s
No. of integrations / blocks, cycles/block	3 / 1 / 50
Blank signal (0.5 M HCl)	0.003 V for ^{195}Pt

The concentration of Pt and other elements was determined using an Agilent 8800 ICP-MS/MS system (Agilent Technologies), using CH_3F and He as reaction/collision gases to avoid spectral interferences. The settings for this instrument can be found in Table II.

TABLE II. Agilent 8800 ICP-MS/MS instrument operating conditions.

Instrument settings	
Sample uptake rate	0.35 mL min^{-1}
Plasma gas flow rate	15.0 L Ar min^{-1}
Auxiliary gas flow rate	0.9 L Ar min^{-1}
Nebulizer gas flow rate	~1.12 L Ar min^{-1}
Collision gas flow rate	1.0 mL He min^{-1}
Reaction gas flow rate	1.00 mL CH_3F/He (10%/90%) min^{-1}
RF power	1550 W
Sample cone	Ni tip with Cu base
Skimmer cone	Ni
Data acquisition parameters	
Integration time	1 s
Replicates	10
Sweeps	100

Results and discussion

Platinum chromatography

Due to isotope fractionation, matrix effects and spectral interferences occurring in MC-ICP-MS instruments, Pt must be isolated prior to isotopic analysis. A number of studies have been published on chromatographic Pt isolation. For example, Creech et al. developed a chromatographic procedure suitable for isolating Pt out of geological reference materials and Poole et al. isolated Pt out of iron meteorites (11,13). Anion exchange column chromatography is the basis for both protocols as Pt forms an anionic complex in dilute HCl (15). These procedures were adapted in order to be viable for biological matrices.

Both Creech et al. and Poole et al. used AG1-X8 anion exchange resin. Contrary to the "heavier" geological samples, the samples used in this research did not contain other Platinum Group Elements and therefore 11 M HCl was not needed for chromatographic Pt isolation during this research. Most matrix elements were eluted using 1 M HCl, except for Zn, which was eluted using 0.8 M HNO_3. Finally, Pt was eluted from the column using concentrated (15.6 M) HNO_3.

A synthetic standard containing elements that can be expected in cell samples was prepared to test and optimize the chromatographic procedure. The amounts of these elements loaded onto the column are found in Table III.

TABLE III. Amount of biologically relevant elements (in µg) loaded onto the column to test the chromatographic procedure.

Element	Loaded onto the column (µg)
Na	0.988
Mg	0.997
K	0.994
Ca	1.010
Fe	0.507
Cu	0.203
Zn	0.503
Pt	0.093

The results of the first test showed that the initially proposed chromatographic procedure could be suited after further optimization and the optimized procedure is shown in Table IV. The corresponding elution profile is shown in Figure 1.

TABLE IV. Optimized chromatographic procedure for Pt isolation out of a biological matrix.

Resin: Bio-rad AG1-X8, 200 – 400 mesh, chloride form, 1 mL

Step	Resin volumes	Eluent
Cleaning	5 mL	H_2O
	5 mL	7.8 M HNO_3
	5 mL	H_2O
	5 mL	7.8 M HNO_3
	5 mL	H_2O
Conditioning resin	5 mL	1 M HCl
Loading sample (cut 1)	1 mL	1 M HCl
Eluting Na, Mg, K, Ca, Fe, Cu (cut 2 - 9)	16 mL (total)	1 M HCl
Eluting Zn (cut 10 – 14)	5 mL (total)	0.8 M HNO_3
Eluting Pt (cut 15 – 19)	20 mL (total)	15.6 M HNO_3

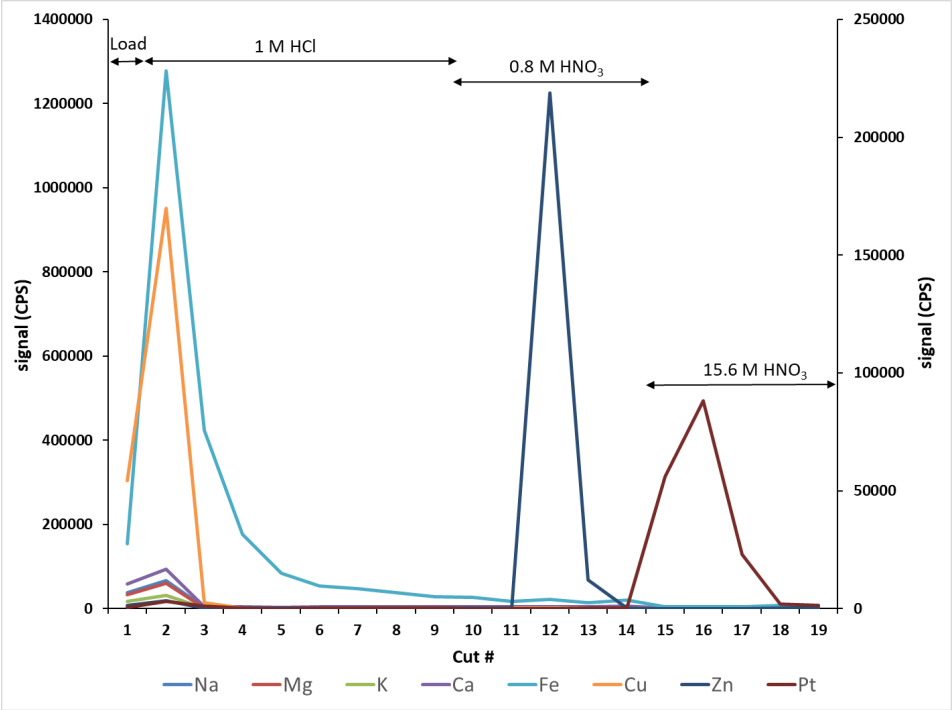

Figure 1. Elution profile for the synthetic sample (composition see Table III) using the optimized chromatographic procedure (Table IV). This shows a good separation of Pt from the other matrix elements, although Fe might be a possible contamination in the Pt fraction.

Influence of contaminating elements and concentration mismatches on Pt isotopic analysis

The next step in the research was developing a measurement protocol to determine Pt isotope ratios using MC-ICP-MS. During this research, the δ^{198}Pt-value for Pt-α was determined. The δ^{198}Pt-values, from now on simply referred to as the δ-values, were calculated according to equation 1.

$$\delta^{198}\mathrm{Pt} = \frac{\left(\frac{^{198}Pt}{^{194}Pt}\right)_{Pt-\alpha} - \left(\frac{^{198}Pt}{^{194}Pt}\right)_{IRMM-010}}{\left(\frac{^{198}Pt}{^{194}Pt}\right)_{IRMM-010}} \cdot 1000(‰) \qquad [1]$$

First of all, sample-standard bracketing combined with internal normalization was tested as a correction procedure. In sample-standard bracketing, unknown samples are measured in-between two measurements of the standard, IRMM-010 in this case. The IRMM-010 ^{198}Pt/^{194}Pt ratio used to calculate the δ-value for the unknown sample is the average of the measured ^{198}Pt/^{194}Pt ratios obtained in the two bracketing standard measurements. Using this average value corrects for drift of the signal over time. This procedure can however not fully correct for temporal drifts in instrumental mass discrimination, but this problem can be addressed by using another element as an internal standard (16). Iridium is ideal for this task due to its occurrence in extremely low quantities in biological materials and it being close in mass to the isotopes of Pt, while suffering no spectral overlap (17).

Results are shown in Figure 2. A combination of internal correction (with Ir) by means of the revised Russell's law and external correction in a sample-standard bracketing approach was used to obtain these results (18). In the first session, using Ir as an internal standard, improved both the accuracy and precision of the δ-value values for Pt-α. Proving that there was potential for this model to work. However, the following measurements, session 2 and session 3, could not reproduce the same results and therefore it was concluded that using Ir as an internal standard to correct Pt isotope ratios did not provide added value. Consequently, regular sample-standard bracketing was used as the correction procedure during this research.

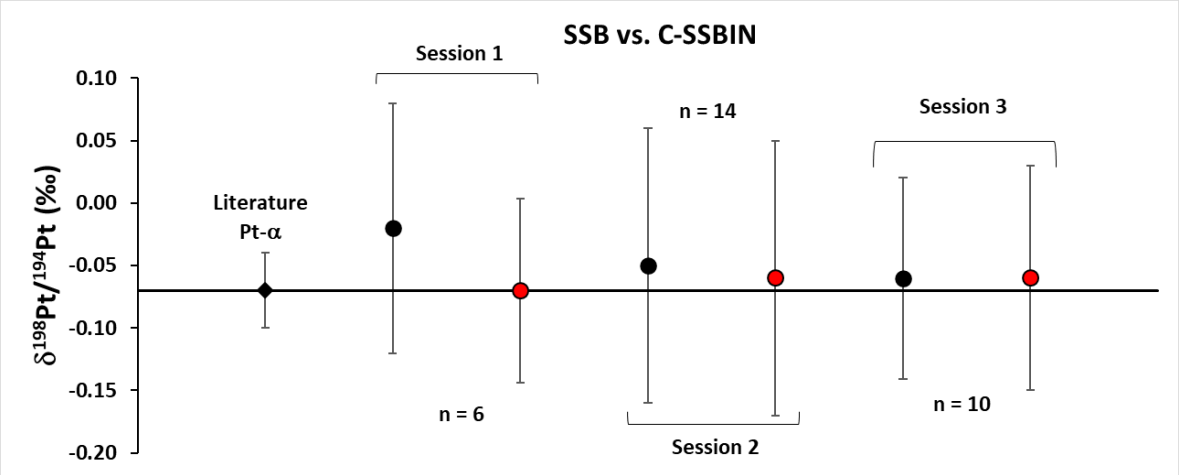

Pt-$\alpha_{IRMM-010}$ = -0.07 ± 0.03 ‰, Poole et al. (13)

Figure 2. Determined δ–values for Pt-α relative to IRMM-010 using sample-standard bracketing (SSB) as a correction procedure (black data points) or using a combination of – sample-standard bracketing with internal normalization (C-SSBIN) with Ir as an internal standard as a correction procedure (red data points). The number of measurements in one session is represented by n. The error bars represent 2 * standard deviation.

After deciding which correction procedure to use, the measurement procedure using the Neptune instrument was tested. If the measurement procedure functioned properly, the δ–value determined for IRMM-010 should be zero since it is calculated relative to itself and the δ-value for Pt-α should be close to -0.07 ± 0.03 ‰ (13)**.** The determined δ-value for IRMM-010 relative to itself was 0.02 ± 0.12 ‰. The average determined δ-value for Pt-α over 7 different measurement sessions was -0.04 ± 0.10 ‰. These results show that the measurements performed during this research provided reliable results, although the precision was worse compared to previous studies. The low precision was likely related to the low Pt concentration in the samples (10 µg/L) and the use of sample-standard bracketing as a correction procedure, instead of double spike correction.

With a proper functioning measurement procedure, the influence of contaminating elements and mismatches of Pt concentrations between sample and bracketing standard on the determined δ-value for Pt-α was examined. Results are shown in Figure 3. The results show that the determined δ-value was not influenced in the measured samples, except possibly for the sample in which the Pt concentration was only 50% of the concentration in the bracketing standard. It should also be noted that, due to working in the clean lab and working as precisely as possible, this level of mismatch or contamination is not expected to be present in the samples.

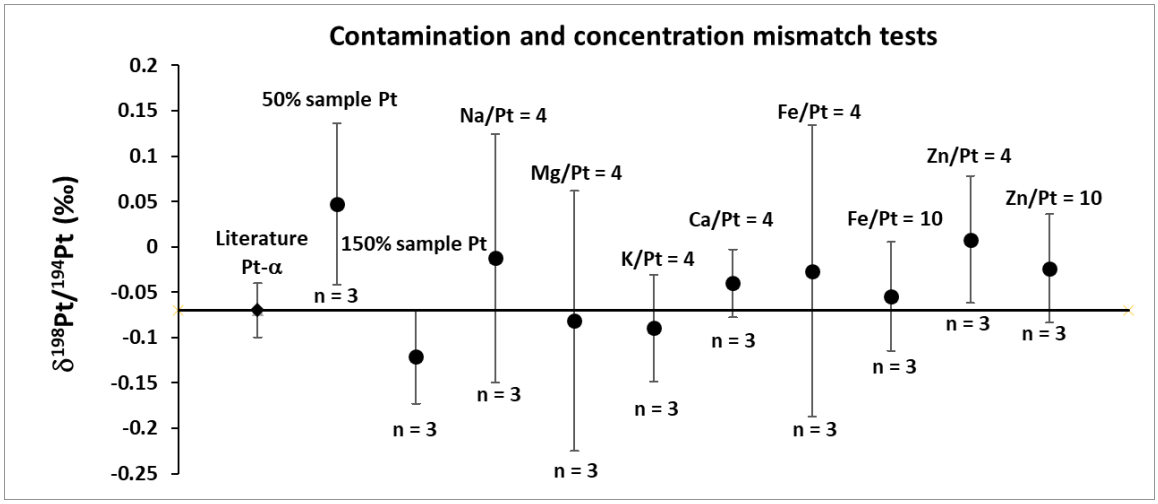

Pt-$\alpha_{IRMM-010}$ = -0.07 ± 0.03 ‰, Poole et al. (13)

Figure 3. Determined δ–values for Pt-α relative to IRMM-010 using SSB as a correction procedure when the Pt concentration in the sample is 50% or 150% of the concentration of Pt in the bracketing standard or when possible contaminants are present in a concentration 4-fold or 10-fold as high as the Pt concentration. The number of measurements in one session is represented by n. The error bars represent 2 * standard deviation.

Isotopic analysis of column cut samples

After evaluating the chromatographic and measurement procedures, it was tested whether the column introduces fractionation. If the column does not cause fractionation effects, the δ-value for Pt-α that did not undergo chromatography should be the same as the δ-value for Pt-α after passing it through a column. For these measurements, both pure Pt-α and a synthetic cell solution (composition see Table V) were passed through a column. It was also tested whether Pt fractions that eluted from the column earlier had a different δ-value than Pt fractions that eluted from the column later on. Column cut samples were treated in the following way: after column chromatography the collected fractions were evaporated to dryness. The resin, that could have come off in the fractions, was destroyed by digesting the fractions in concentrated HNO_3 on a hotplate overnight, after which the samples were evaporated to dryness once again. Then they were digested in 6 M HCl on a hotplate overnight, to convert the samples into chloride form after which the digest was evaporated to dryness one more time to finally obtain a solution in 0.5 M HCl to be measured on the Neptune. Results are shown in Figure 4.

TABLE V. Amount of biologically relevant elements (in µg) loaded onto the column (present in the synthetic cell solution). This synthetic cell solution was prepared to match the amount of the elements that are expected to be in the ovarian cancer cell samples.

Element	Loaded onto the column (µg)
Na	265.130
Mg	14.179
K	106.973
Ca	3.693
Fe	0.374
Cu	0.054
Zn	1.287
Pt	0.098

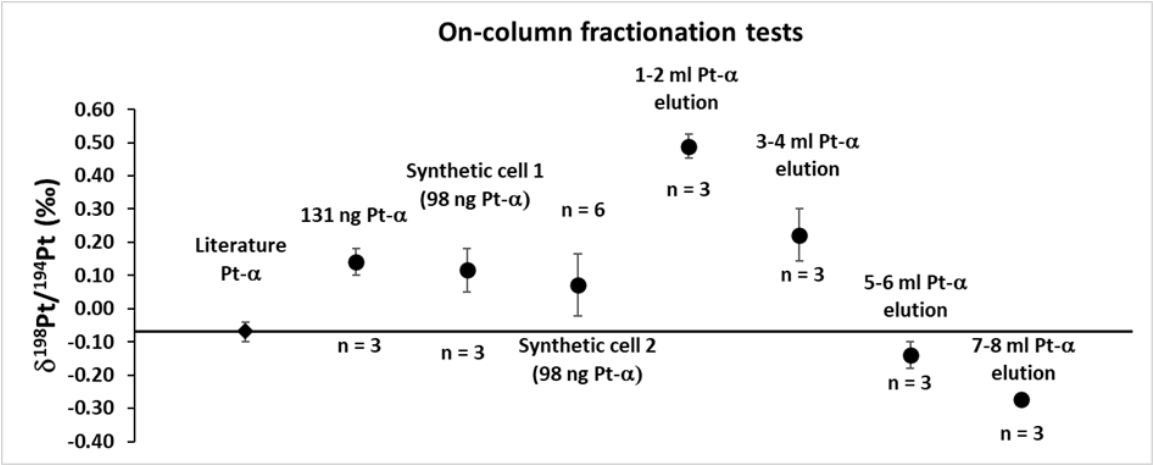

Pt-$\alpha_{IRMM-010}$ = -0.07 ± 0.03 ‰, Poole et al. (13)

Figure 4. Determined δ-values for Pt-α relative to IRMM-010 for samples that were passed through a column. The first three tests provided values for the entire Pt fraction (the 15.6 M HNO_3 fraction) of samples loaded onto a column. The final four values all stem from one chromatographic separation and represent the δ-value in the cuts collected in a smaller volume (2 mL). The number of measurements in one session is represented by n. The error bars represent 2 * standard deviation.

The δ-value for Pt-α was significantly higher when the Pt was passed through a column (around 0.20 ‰ higher). The δ-values for the pure Pt-α solution and the synthetic cell solution were in the same range, suggesting that the other elements present in the synthetic cell solution did not influence the measurement. A possible explanation for the observation can be given by evaluating the results for 1500 ng Pt-α processed on the column and collected in 2 mL cuts instead of 4 mL cuts. The δ-value for the first cut is higher (0.49 ± 0.04 ‰) than the δ-value for the fourth cut (-0.27 ± 0.01 ‰), which suggests that the heavier isotopes of Pt are eluted first. Therefore, if some Pt would be left on the column, it would be enriched in the lighter isotopes, explaining why the δ-values for Pt-α that was passed through a column were higher. However, the elution profile indicated quantitative Pt recovery from the column. This suggests that not only the heavy isotopes were eluted from the column, but the lighter ones as well. Thus, the explanation given cannot be correct.

Due to this observation, new samples were processed on the column, including the IRMM-010 standard reference material. The reference material processed through a column was used as a bracketing standard for the Pt-α samples that were passed through a column. In this way, the matrix of both samples was essentially matched and the δ-value determined for Pt-α should be closer to the value reported in literature. These column-processed samples were also treated with more steps post-column, in order to definitely avoid organic contamination originating from the resin. First, the samples were evaporated to dryness and then digested in aqua regia, a mixture of 3:1 volume ratio of concentrated (10.6 M) HCl : concentrated (15.6 M) HNO_3, on a hotplate overnight, instead of just digesting in concentrated HNO_3. The samples were then evaporated to dryness once again and then digested in a mixture of concentrated HNO_3 and H_2O_2 (3:1 volume ratio) on a hotplate overnight. Once more, the samples were evaporated to dryness. Then the samples were digested in 6 M HCl on a hotplate overnight, to convert them into chloride form after which the digest was evaporated to dryness one more time to finally obtain a solution in

0.5 M HCl to be measured on the Neptune. The results are summarized in Figures 5.a,b and c. The sample names show how much Pt-α or IRMM-010 was loaded onto the column.

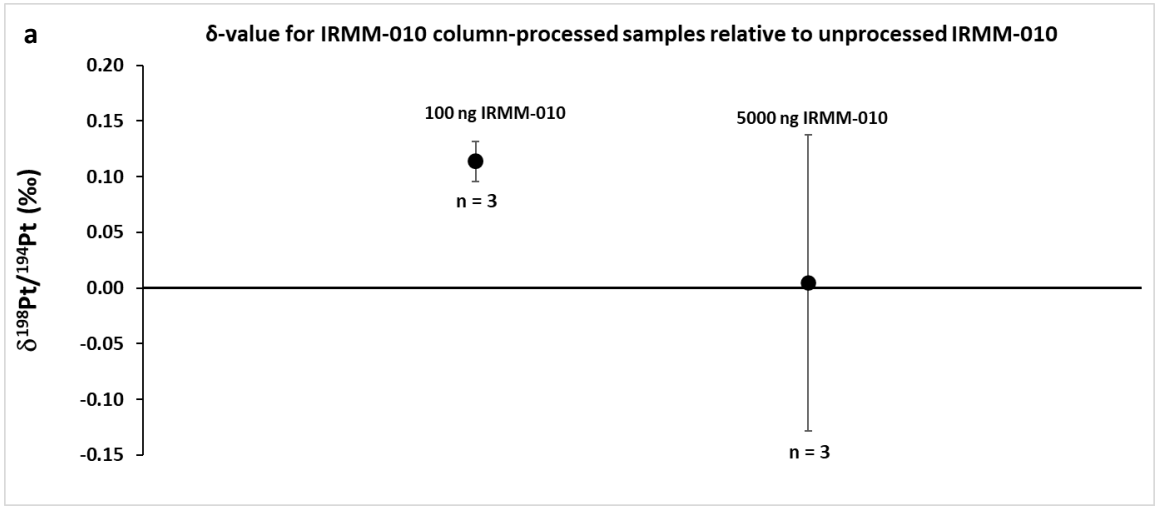

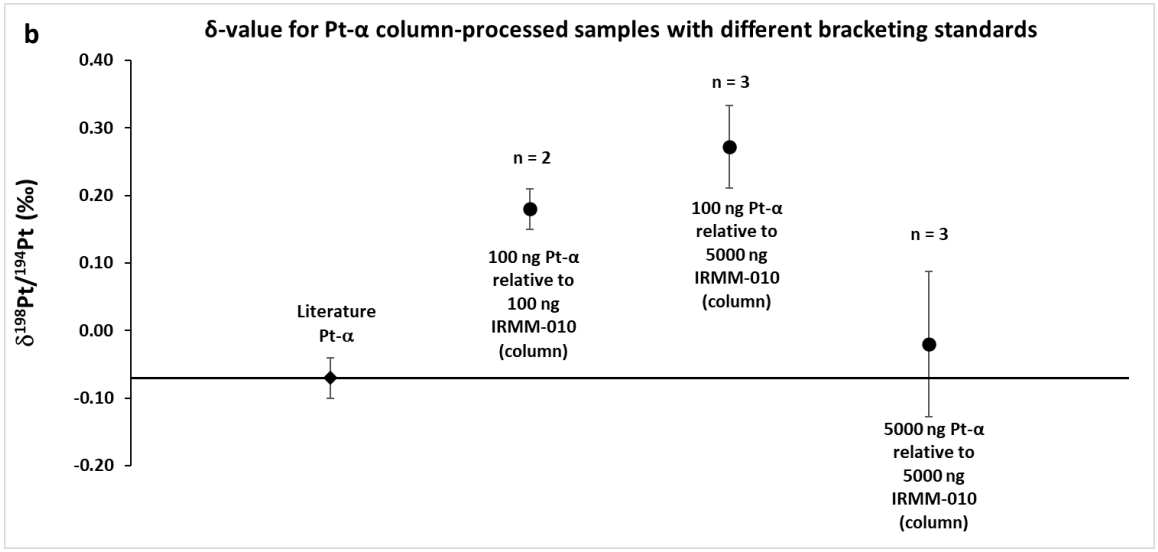

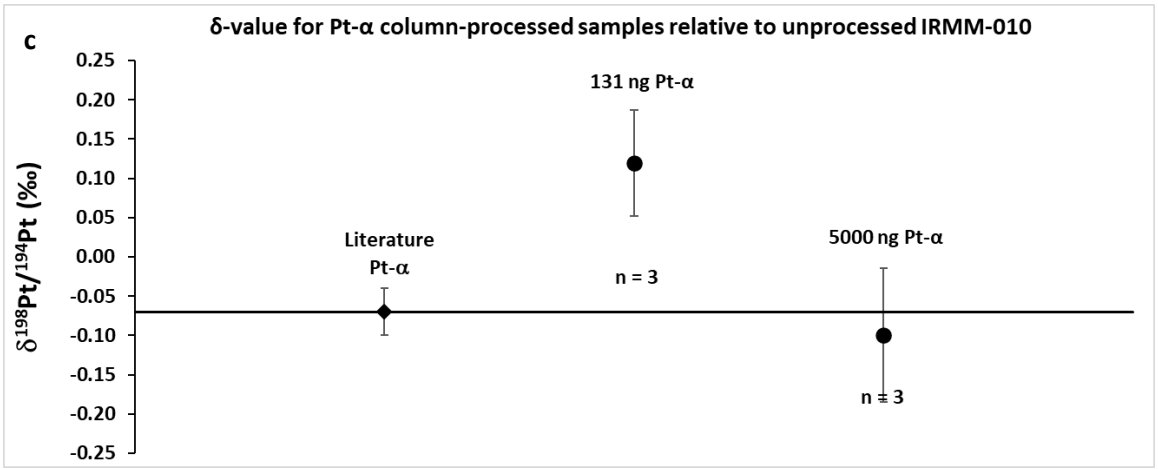

Figure 5. **a** δ-values for IRMM-010 samples that were passed through a column relative to IRMM-010 that was not passed through a column. Absence of on-column fractionation would mean that this value is around 0.00 ‰. **b** δ-values for Pt-α samples that were passed through a column relative to different bracketing standards that were passed through a column. **c** δ-values for Pt-α samples that were passed through a column relative to IRMM-010 that was not passed through a column.

The combined results obtained until now suggest that higher δ-values are obtained when smaller amounts of Pt are loaded onto the column. To confirm this observation, the 5000 ng Pt-α sample was measured against IRMM-010 that was not passed through a column as bracketing standard. The δ-value measured for the 5000 ng Pt-α sample was -0.10 ± 0.09 ‰, which is similar to the result for Pt-α that was not processed on the column and the literature value. According to this result, the column did not cause fractionation effects when a higher amount of Pt-α was loaded onto the column. For comparison, Figure 5b also includes the result of a previous test, in which only 131 ng Pt-α was loaded onto the column and the δ-value was also calculated relative to IRMM-010 that was not passed through a column.

These column samples were also analyzed using the Agilent 8800 ICP-MS/MS instrument to determine whether the column introduced an unknown contamination which could have influenced the results. The contaminant / Pt ratio was then determined. However, no ratio was higher than 0.70 and earlier results indicated that even a 4.00 concentration ratio did not influence the measured δ-value.

Summary

This research set out to determine whether resistance to cisplatin affects Pt isotope fractionation in ovarian cancer cells. Due to the limited availability of cell samples, the measurement procedure had to be developed, optimized and validated before analyzing actual samples. A chromatographic procedure for isolation of Pt out of a biological matrix was successfully developed. δ-values for Pt-α in synthetic samples were determined to check the possibility of using Ir as an internal standard for correction and to examine the influence of contaminants and concentration mismatches between samples and bracketing standard. Loading a small amount of Pt onto the column was observed to influence the δ-value. The precision achieved during this research was also worse compared to previous research, so different correction procedures e.g. the double spike correction could possibly improve results as well. Ultimately, the final goal of determining whether resistance to cisplatin affects Pt isotope fractionation in ovarian cancer cells was not reached. This research does however provide a solid basis for future research in Pt isotopic analysis in the context of ovarian cancer

Acknowledgments

I would like to thank Kaj V. Sullivan (A&MS – Ghent University) for the valuable guidance and supervision during the research and for helping me with the writing part as well. I would also like to thank Frank Vanhaecke and the whole A&MS research group for allowing me to work in the clean lab and use the (MC-)ICP-MS instruments at their disposal.

References

1. Dawson, T. E.; Brooks, P. D. Fundamentals of stable isotope chemistry and measurement. *Stable isotope techniques in the study of biological processes and functioning of ecosystems*, 1-18 (2001).
2. Albarède, F. Metal stable isotopes in the human body: a tribute of geochemistry to medicine. *Elements*, *11* (4), 265-269 (2015).
3. Mahan, B.; Chung, R. S.; Pountney, D. L.; Moynier, F.; Turner, S. Isotope metallomics approaches for medical research. *Cellular and Molecular Life Sciences*, *77* (17), 3293-3309. DOI: 10.1007/s00018-020-03484-0 (2020).
4. Sullivan, K. V.; Moore, R. E. T.; Vanhaecke, F. The influence of physiological and lifestyle factors on essential mineral element isotopic compositions in the human body: implications for the design of isotope metallomics research. *Metallomics*, *15* (3). DOI: 10.1093/mtomcs/mfad012 (acccessed 4/30/2023) (2023).
5. van Zyl, B.; Tang, D.; Bowden, N. A. Biomarkers of platinum resistance in ovarian cancer: what can we use to improve treatment. *Endocrine-related cancer*, *25* (5), R303-R318 (2018).
6. Kilari, D.; Guancial, E.; Kim, E. S. Role of copper transporters in platinum resistance. *World journal of clinical oncology*, *7* (1), 106 (2016).
7. Krizkova, S.; Ryvolova, M.; Hrabeta, J.; Adam, V.; Stiborova, M.; Eckschlager, T.; Kizek, R. Metallothioneins and zinc in cancer diagnosis and therapy. *Drug Metabolism Reviews*, *44* (4), 287-301 (2012).
8. Kischel, P.; Girault, A.; Rodat-Despoix, L.; Chamlali, M.; Radoslavova, S.; Abou Daya, H.; Lefebvre, T.; Foulon, A.; Rybarczyk, P.; Hague, F. Ion channels: New actors playing in chemotherapeutic resistance. *Cancers*, *11* (3), 376 (2019).
9. Schoeberl, A.; Gutmann, M.; Theiner, S.; Corte-Rodríguez, M.; Braun, G.; Vician, P.; Berger, W.; Koellensperger, G. The copper transporter CTR1 and cisplatin accumulation at the single-cell level by LA-ICP-TOFMS. *Frontiers in Molecular Biosciences*, 1303 (2022).
10. Cadiou, J.-L. Copper transporters are responsible for copper isotopic fractionation in eukaryotic cells. PhD thesis, Université de Lyon (2017).
11. Creech, J. B.; Baker, J. A.; Handler, M. R.; Bizzarroc, M. Platinum stable isotope analysis of geological standard reference materials by double-spike MC-ICPMS. *Chemical Geology*, *363*, 293-300. DOI: 10.1016/j.chemgeo.2013.11.009 (2014).
12. Creech, J.; Baker, J.; Handler, M.; Lorand, J.-P.; Storey, M.; Wainwright, A.; Luguet, A.; Moynier, F.; Bizzarro, M. Late accretion history of the terrestrial planets inferred from platinum stable isotopes. *Geochem. Perspect. Lett*, *3*, n1 (2017).
13. Poole, G. M.; Stumpf, R.; Rehkämper, M. New methods for determination of the mass-independent and mass-dependent platinum isotope compositions of iron meteorites by MC-ICP-MS. *Journal of Analytical Atomic Spectrometry*, *37* (4), 783-794 (2022).
14. Breton, T.; Lloyd, N. S.; Trinquier, A.; Bouman, C.; Schwieters, J. B. Improving precision and signal/noise ratios for MC-ICP-MS. *Procedia Earth and Planetary Science*, *13*, 240-243 (2015).

15. Pearson, D.; Woodland, S. Solvent extraction/anion exchange separation and determination of PGEs (Os, Ir, Pt, Pd, Ru) and Re–Os isotopes in geological samples by isotope dilution ICP-MS. *Chemical Geology*, *165* (1-2), 87-107 (2000).
16. Yang, L.; Tong, S.; Zhou, L.; Hu, Z.; Mester, Z.; Meija, J. A critical review on isotopic fractionation correction methods for accurate isotope amount ratio measurements by MC-ICP-MS. *Journal of Analytical Atomic Spectrometry*, *33* (11), 1849-1861 (2018).
17. Zhu, Z.; Meija, J.; Zheng, A.; Mester, Z.; Yang, L. Determination of the isotopic composition of iridium using multicollector-ICPMS. *Analytical Chemistry*, *89* (17), 9375-9382 (2017).
18. Baxter, D. C.; Rodushkin, I.; Engström, E.; Malinovsky, D. Revised exponential model for mass bias correction using an internal standard for isotope abundance ratio measurements by multi-collector inductively coupled plasma mass spectrometry. *Journal of Analytical Atomic Spectrometry*, *21* (4), 427-430 (2006).

Page left intentionally blank

Contents

References

1. Introduction

Isotopes of an element are atoms with the same number of protons, but a different number of neutrons in the nucleus. That is, they have the same atomic number, but a different mass number.[1] The abundance of isotopes for a given element are mostly constant in nature, but can vary slightly when radionuclides decay into daughter products, or when stable isotopes undergo a change in bonding environment (phase change, oxidation state, coordination number, ligand chemistry) accompanied by isotope fractionation.[2]

The term "isotopic fractionation" refers to the relative partitioning of "heavy" (higher mass) and "light" (lower mass) isotopes between two coexisting phases in a system. Natural variations in stable metal isotope ratios (heavy/light) occur in nature due to the "isotope effect". This term explains mass-dependent variation in natural isotopic abundances as a consequence of the fact that the lowest vibrational energy state depends on the mass of the atoms involved in bonding. As heavier isotopes vibrate more slowly than the lighter ones (i.e. their vibrational frequency is lower) and bond energy is inversely proportional to vibrational frequency, heavier isotopes tend to occupy the lowest, most stable energy levels (i.e. stronger bonds).[3] So, when one isotope substitutes for another in a chemical bond, a change in energy occurs due to the difference in mass between the isotopes.[4] As a consequence, isotopes will redistribute as a function of their mass, a phenomenon which is called mass-dependent isotope fractionation. This property is used in the field of *biomedical isotopic analysis*, where variations in bodily stable metal isotope ratios are studied in the context of biomedicine.[3] *Biomedical isotopic analysis* emerged from the development of multi-collector inductively coupled mass spectrometry (MC-ICP-MS), a technique initially developed for applications in geo- and cosmochemistry. High-precision isotopic analysis by MC-ICP-MS allows for the simultaneous measurement of multiple mass-to-charge ratios, significantly improving isotope ratio precision.[4] High-precision isotopic analysis by MC-ICP-MS is considered promising for both the elucidation of processes involved in metal dysregulation, and as a biomarker for the diagnosis and prognosis of diseases.[5]

Metal dysregulation is often inherent to cancers and other diseases and can result in systemic changes to essential mineral element (Mg, K, Ca, Fe, Cu and Zn) stable isotopic compositions.[6] This discovery has led to research on stable isotope ratio-based biomarkers, and has even resulted in several spin-off companies. For example, Osteolabs GmbH, which offers the measurement of urine and blood Ca isotope ratios for the early detection of osteoporosis.[6]

Early diagnosis often plays an important role in determining cancer treatment outcomes, but the diagnosis of ovarian cancer poses significant challenges, and the routine screening of asymptomatic average-risk women is not recommended by any professional society.[7] In part due to the low incidence of ovarian cancer, the screening of average-risk women with the most common biomarker, serum Cancer Antigen 125 (CA125) levels, results in a significant number of false positives.[8] Additionally, about 20% of ovarian cancers have no CA125 expression.[9, 10] As a result, average-risk asymptomatic women screened with an annual transvaginal ultrasound and CA125 tests indicated no mortality reduction compared to women receiving standard care after a median of 15 years of follow-up.[11] Serum CA125 has a role in routine clinical care of ovarian cancer patients for evaluating therapeutic

efficacy and monitor disease status,[12] but methods to assess cancer drug resistance are still in their infancy, with none approved for clinical use yet.[13] The ability to predict patient response towards post-operative treatments would allow for ineffective treatments and harmful side effects to be avoided and alternative treatments to be commenced at earlier stages.

Chemotherapy using Pt-based compounds (e.g. carboplatin, cisplatin) is a standard treatment, but tumours that are initially responsive may develop chemoresistance, resulting in treatment failure.[14] Patients treated with chemotherapy can be categorized as either sensitive or resistant based on the time from the end of the treatment to relapse. Several mechanisms underlying tumour cell resistance have been identified so far, including the altered expression of ion channels (Na, Mg, K, and Ca) and Fe-, Cu-, and Zn-binding proteins, but these remain poorly understood and it is unclear whether they can be exploited as markers of resistance.[15-17] However, there is a significant correlation between high-affinity Cu uptake protein 1 (CTR1) expression and cisplatin accumulation in the A2780 and A2780cis ovarian cancer cell lines, demonstrating a link between Cu homeostasis and cisplatin uptake.[18] Altered Cu homeostasis has also been demonstrated in four strains of cisplatin-resistant yeast, with the decreased expression of CTR1 being associated with increased $^{65}Cu/^{63}Cu$ values, demonstrating the potential of isotopic analysis as a marker of chemoresistance.[19] Platinum has 6 naturally occurring isotopes: ^{190}Pt, ^{192}Pt, ^{194}Pt, ^{195}Pt, ^{196}Pt and ^{198}Pt, with abundances of ~ 0.01%, 0.78%, 32.86%, 33.78%, 25.21%, and 7.36%, respectively.[20] Although Pt isotopic analysis finds application with helping to constrain terrestrial core formation and other geochemical processes, it is yet to be applied in a biomedical context.[20-22] However, it is common for cancers, such as ovarian cancer, to develop resistance during the prolonged treatment process, and a strong case can be made for investigating whether the Pt isotopic composition of the drug reaching the affected cells is altered when its normal functioning is disrupted. The interaction of the Pt drug with Pt-based chemotherapeutic drug-resistant ovarian cancer cells would be associated with changes to Pt speciation and binding, and these may be detected via Pt isotopic analysis.

With the aim of revealing mechanisms behind Pt-based chemotherapeutic drug resistance and identifying novel markers of chemoresistance, I will determine whether changes in the natural abundances of Pt isotopes are associated with the development of resistance to Pt-based chemotherapeutic drugs in chemoresistant (A2780cis) and chemosensitive (A2780) ovarian cancer cell lines. It will also be explored whether any change in the Pt isotopic composition between chemosensitive and chemoresistant cells is reflected in the growth medium with a compensatory Pt isotopic signature, as this could be analogous to a change in Pt isotopic composition being induced in blood upon the development of chemoresistance. The finding of biologically induced Pt isotopic fractionation would validate this proof-of-concept and could lead to several avenues of research to explore beyond this thesis. These could include the Pt isotopic analysis of patient-derived tumour fragments, which is an opportunity to study the baseline properties of the tumour and initial chemotherapeutic response. There is also the possibility of assessing blood Pt isotopic compositions after initial drug administration as a marker of chemoresistance. If patients who would not respond to Pt-based chemotherapeutic drugs can be identified before or shortly after commencing treatment, potentially harmful side-effects can be avoided and alternative treatments with the chance of helping the patient can be implemented earlier.

2. State-of-the-art:

The study of variations in stable metal isotope ratios in a biomedical context can be referred to as the field of *biomedical isotopic analysis*. This section will include discussion on the state-of-the-art of relevant topics, such as the instrumentation (MC-ICP-MS, tandem ICP-MS), chromatographic Pt isolation and similar studies of essential mineral element isotopic fractionation (Ca, Cu). Since carboplatin and cisplatin are the compounds that will be studied, a deeper look into their properties and mechanisms of action will also be included.

2.1 Instrumentation

2.1.1 ICP-MS

The term ICP-MS is a combination of two things: ICP refers to inductively coupled plasma, which is the source used to break down the sample and convert it into atomic ions in order to determine its elemental composition by mass spectrometry (MS). This ionization is a necessary step because mass spectrometry cannot measure neutral atoms.[23] Figure 1 (Linge, 2009) shows a schematic diagram of a quadrupole based ICP-MS system, which is the most common commercially available system.

A liquid sample is first converted into a form that is compatible with the plasma (most commonly an aerosol) through the use of a nebulizer and spray chamber, and it is ensured that only a fine spray of droplets reaches the plasma. The plasma is a gas mixture of ions, electrons and neutral atoms and molecules at a high temperature. It has sufficient energy to remove electrons from atoms of the sample, which leads to production of atomic ions for mass analysis. Since the plasma operates at

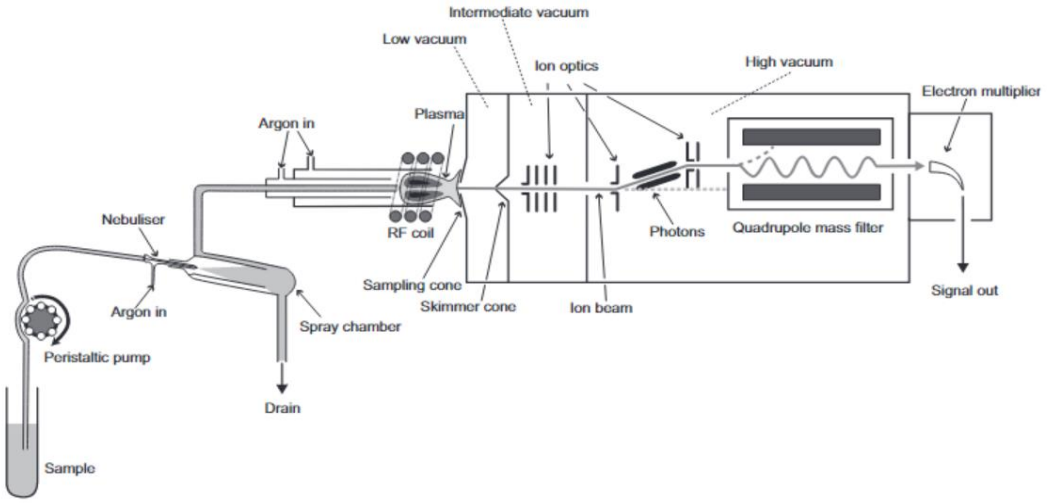

Figure 1 Schematic overview of a quadrupole-based ICP-MS system (Linge, 2009).

atmospheric pressure and the mass spectrometer operates under vacuum, an interface region is also needed. Photons are also removed after this interface through ion optics steering the ion beam. In quadrupole ICP-MS, this region is then followed by the quadrupole filter and a detector.[23] However, in MC-ICP-MS units this is slightly different (Figure 2) (Greber, 2022).

2.1.2 MC-ICP-MS

Instead of a quadrupole, an MC-ICP-MS instrument contains an electrostatic analyzer, followed by a magnetic sector analyzer. In sector field mass spectrometry, ions are separated based on their mass-to-charge (m/z) ratio by the magnetic sector analyzer. However, to some extent, the plasma produces ions with the same m/z ratio that differ in their kinetic energy and this negatively affects the mass differentiation. The electrostatic analyzer compensates for this difference and preserves mass resolution. The separated ions with different m/z ratio are finally detected simultaneously by an array of detectors as opposed to a single one. This simultaneous measurement is the reason why isotope ratios can be measured so accurately and precisely by MC-ICP-MS.[24]

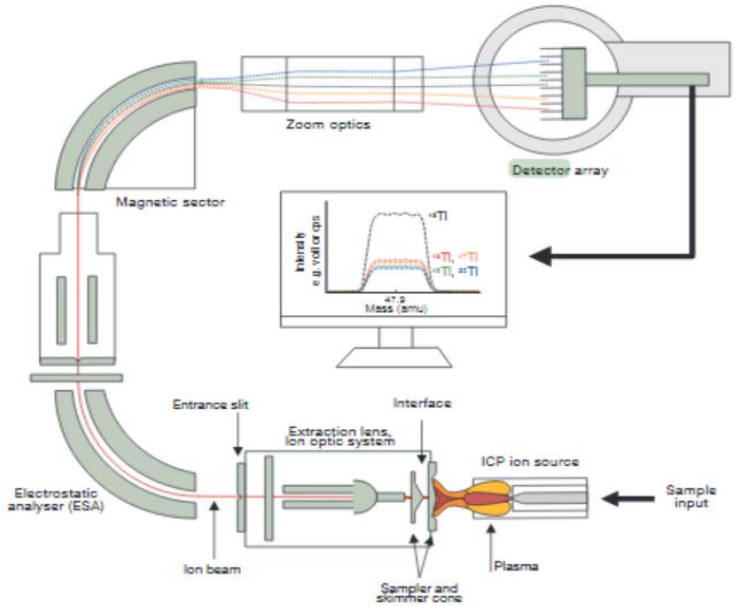

Figure 2 Schematic overview of an MC-ICP-MS instrument (Greber, 2022)**.**

In this thesis isotope ratios of Pt in different samples will be measured to see if there is a shift in Pt isotope abundances between chemoresistant and chemosensitive cells. Shifts in isotope abundance are typically very small and therefore expressed as delta(δ) values. Δ-values are always calculated relative to a standard or reference material.

$$\Delta = \frac{\left(\frac{^{h}X}{^{l}X}\right)_{sample} - \left(\frac{^{h}X}{^{l}X}\right)_{reference}}{\left(\frac{^{h}X}{^{l}X}\right)_{reference}} \cdot 1000(‰) \qquad \text{[Equation 1]}$$

δ-values are calculated according to Equation 1, where X represents the element of interest, h in the superscript is the mass of the heavy isotope and l in the superscript refers to the mass of the light isotope of the element of interest. They are multiplied by 1,000 and reported in ‰ values.[25]

2.1.3 Tandem ICP-MS

During this thesis, especially during the chromatographic isolation of Pt, it will be relevant to measure concentrations of essential mineral elements (Na, Mg, K, Ca, Fe, Cu and Zn) that are present in the sample. In order to accomplish this, tandem ICP-MS will be used. Tandem ICP-MS is based on the same basic principles as all the other types of ICP-MS, but removes spectral interferences more efficiently. The first mass filter, a quadrupole, only lets ions with the selected m/z ratio go through. Isobaric or polyatomic interferences at the same m/z as the analyte of interest are then avoided by relying on physicochemical processes in a collision/reaction cell, where either the analyte of interest or the interferences interact with an adequately selected gas. After this interaction, there is a final mass filter that is set to a suitable m/z ratio for monitoring the analyte of interest. This can be the same m/z ratio as the first filter if the interfering ions react with the cell gas, or it is set to the m/z ratio of the reaction product ion created by reaction between the cell gas and the analyte of interest (Figure3).[26] Figure 3 (Balcaen, 2015) shows the advantage of using two mass filters.

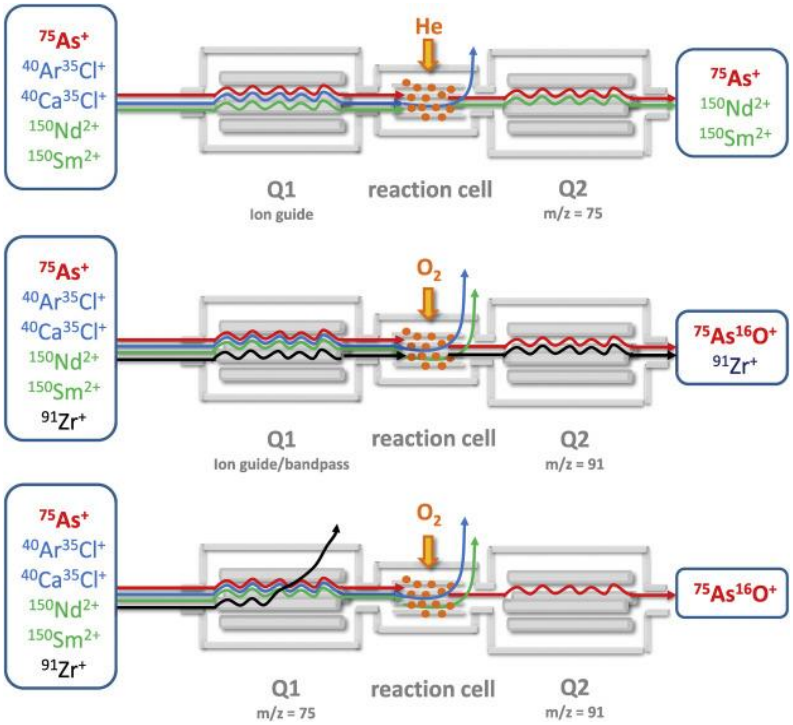

Figure 3 Three different setups that show the power of tandem ICP-MS, also known as ICP-MS/MS (Balcaen, 2015).

In the first setup, all ions pass the first quadrupole and polyatomic interferences are removed because of collision with the He, which causes them to lose kinetic energy such that they lack sufficient energy to enter the second mass filter. However, the interfering doubly charged ions remain present, as they do not collide at the same rate with He due to their smaller size. This is true for all monoatomic interferences, not just those that are doubly charged. In the second setup, these doubly charged ions are removed by the second mass filter because the m/z ratio of this filter is set to 91 and the m/z ratio of the analyte of interest is shifted to 91, but since all ions were allowed to pass the first filter, there is now interference with ^{91}Zr. The third setup shows the power of tandem ICP-MS. The $^{91}Zr^{+}$ ions are filtered out before the reaction cell because the first quadrupole only allows ions of m/z = 75 to pass. After the first mass filter, the analyte reacts with the reaction gas, creating the only ion present at m/z = 91. The second filter then only lets the analyte of interest at the new m/z ratio pass, allowing for a more accurate and interference-free measurement.[26]

2.2 Previous research based on Pt isotopic analysis

As mentioned in the introduction, platinum has 6 naturally occurring isotopes: ^{190}Pt, ^{192}Pt, ^{194}Pt, ^{195}Pt, ^{196}Pt and ^{198}Pt, with abundances of ~ 0.01%, 0.78%, 32.86%, 33.78%, 25.21%, and 7.36%, respectively. Whereas ^{190}Pt is not a stable isotope, it has an extremely long half-life of 10^{11} years.[20] The applications of Pt isotopic analysis are wide-ranging. So far, Pt isotope ratios have been used in applications, as aiming at helping to constrain terrestrial core formation and the late addition of extra-terrestrial materials to the Earth's mantle, tracing redox processes in marine environments, and tracing vehicular emissions, among others.[20-22] However, Pt isotopic analysis is yet to be applied in a biomedical context. Given the ubiquity of Pt-based chemotherapeutic drugs in the treatment of cancers, and that it is common for cancers, such as ovarian cancer, to develop resistance during the prolonged treatment process, there may be potential induction of changes in the Pt isotopic composition of the Pt drug reaching the affected cells upon the development of chemoresistance.

2.2.1 Chromatographic isolation of Pt

Due to isotopic fractionation, matrix effects and spectral interferences occurring in MC-ICP-MS instruments, Pt must be isolated prior to isotopic analysis. A number of studies have been published on chromatographic Pt isolation. For example, Creech et al. developed a chromatographic protocol suitable for isolating Pt out of geological reference materials and Poole et al. isolated Pt out of iron meteorites.[20, 22] Anion exchange column chromatography is the basis for both protocols as Platinum Group Elements (PGEs), which Pt is a part of, form anionic complexes in dilute HCl.[27] These methods will form the basis of the protocol adapted towards a more biomedical context.

In chromatography, substances are separated based on their affinity for two different phases, a stationary and a mobile phase. When the substance shows no interaction with the stationary phase, it is eluted from the column first. The mobile phase can then be altered in composition in order to elute other substances that remained (showed interaction with the stationary phase) on the column. Anion exchange chromatography is a form of ion exchange chromatography, where substances are separated based on electrostatic interactions.[28] In anion exchange chromatography, the stationary phase (or resin) is net positively charged and thus Pt anionic complexes formed in dilute HCl are attracted and retained by the stationary phase.

There are several steps in a general ion exchange chromatography procedure that are also described in the studies by Creech et al. and Poole et al. The resin first has to be cleaned several times to remove the fine particles (by rinsing with a suited solvent and decanting) and then loaded into the column. After the resin has settled, it is further cleaned to remove contaminants. Before loading the sample, the column is conditioned by letting a solvent (mixture) pass the resin, in these cases the solvent (mixture) in which the sample is dissolved. The sample is loaded onto the column and then several solvents, or eluents, are used as mobile phase to separate the different compounds from one another. Chromatographic methods can be evaluated and optimized by collecting different fractions in order to define when the matrix elements and analyte leave the column.

2.2.2 Adaptation of chromatographic isolation of Pt for biological samples

The chromatographic procedure to be used this project will be adapted from the procedures shown in Table 1a and 1b. Our biological samples will not contain PGEs, so the use of concentrated (11 M) HCl will not be necessary. 1 M HCl will be used to elute most of the matrix elements, except Zn, which is removed with 0.8 M HNO_3. Pt is collected using concentrated (14 M) HNO_3. A more detailed description of the chromatographic procedure, including amounts of volume, can be found in the work packages section.

Table 1a Chromatographic procedure for Pt isolation used by Creech et al.[20]

Resin: Bio-Rad AG1-X8, 100 -200 mesh, chloride form, 1 mL		
Step	Resin volumes	Acid
Cleaning	20 mL	0.8 M HNO_3
	10 mL	11 M HCl
	25 mL	13.5 M HNO_3
	40 mL	6 M HCl
Pre-conditioning resin	40 mL	0.5 M HCl
Loading sample	10 mL	0.5 M HCl
Eluting matrix	40 mL	0.5 M HCl
	20 mL	1 M HCl
Eluting Zn	20 mL	0.8 M HNO_3
Eluting PGEs	60 mL	11 M HCl
Eluting Pt	40 mL	13.5 M HNO_3

Table 1b Chromatographic procedure for Pt isolation used by Poole et al.[22]

Resin: Bio-Rad AG1-X8, 200 -400 mesh, chloride form, 1 mL		
Step	Resin volumes	Acid/solvent
Cleaning	1.5 mL	8 M HNO_3
	1 mL	H_2O
	1.5 mL	11 M HCl
	1 mL	1 M HCl
Pre-conditioning resin	4 mL	1 M HCl
Loading sample	2 – 4 mL	1 M HCl
Eluting matrix (Fe, Ni)	40 mL	0.5 M HCl
Eluting PGEs	50 mL	11 M HCl
	1 mL	H_2O
Eluting Pt	14 mL	13.5 M HNO_3

2.3 Applications of biomedical isotopic analysis

2.3.1 Ca isotopic analysis in bone diseases

The power of measuring stable isotopes in a biomedical context can be illustrated using a study by Morgan et al. In this study, Ca stable isotopes ratios are used to rapidly determine a change in the bone mineral balance (BMB).[29]

In humans, bone is constantly replaced by a process involving both bone-forming cells (osteoblasts) and bone resorbing cells (osteoclasts). When an adult individual is healthy, the rate of formation of bone is equal to the rate of bone resorption. In this case the bone mineral balance (BMB) is equal to zero. In an unhealthy individual that suffers from a bone disease such as osteoporosis, the BMB can be disrupted, meaning the formation rate might exceed the resorption rate (positive BMB) or the resorption rate might exceed the formation rate (negative BMB). Eventually, this disruption may lead to a change in bone mineral density that can be measured by x-ray densitometry, but a change which can be measured takes months or even years. Calcium isotopic analysis can detect changes in bone mineral density after just one week.[29]

It was already established that isotopes will fractionate in certain processes based on their atomic mass due to the isotope effect. In the context of BMB, there are two processes that lead to changes in Ca isotope abundances. Firstly, when bone is formed, lighter isotopes of Ca are preferably taken up from soft tissue (blood and non-bone tissue). In contrast to this, in bone resorption there is no preference for either light or heavy isotopes, so every isotope is released into the soft tissue without isotope selectivity. This means that when bone formation exceeds bone resorption (positive BMB), Ca isotope abundances in soft tissue shift to a heavier Ca isotopic composition. Secondly, heavier isotopes are preferably excreted by the kidneys. This mechanism of fractionation is not that well understood, but once again when the BMB is positive, less Ca is excreted, and the Ca isotopic composition in soft tissue shifts to a heavier isotopic composition. Urine samples can thus also be measured as shifts in the Ca isotopic composition in soft tissue are correlated to shifts in the Ca isotopic composition in urine.[29]

2.3.2 Cu isotopic analysis in ovarian cancer research

Recent work has shown that the Cu isotope ratio shows potential for use as a biomarker of ovarian cancer. As mentioned earlier, the diagnosis of ovarian cancer poses significant challenges, and the routine screening of asymptomatic average-risk women is not recommended by any professional society. The serum copper isotopic composition of breast cancer patients has been investigated and there was a strong correlation between the $\delta^{65}Cu$ value and cancer development. Due to this correlation, the $^{65}Cu/^{63}Cu$ ratios in samples from ovarian cancer patients were also investigated by Toubhans et al. to evaluate whether monitoring the Cu isotope ratio is also meaningful in this type of cancer.[30]

In the study, both serum and tissue samples of ovarian cancer patients were compared to samples from healthy individuals. The $\delta^{65}Cu$ value in serum of ovarian cancer patients was significantly lower than the value in serum of healthy individuals and the opposite was found in the tissue samples due to the preferential uptake of ^{65}Cu.[30]

It has been suggested that the decrease of the $\delta^{65}Cu$ value in serum and the increase of the $\delta^{65}Cu$ value in tumour tissue is a consequence of the hypoxic environment of tumour tissue. This type of environment relatively increases the amount of lactate compared to healthy tissue.[30] Lactate is a metabolic waste product that is produced when there is higher demand for ATP and oxygen than there is supply.[31] The structure of lactate is shown in Figure 4 which shows that a carboxyl group is present. This carboxyl group is responsible for the isotope fractionation. The heavy ^{65}Cu atoms form more stable bonds with the carboxyl group than the light ^{63}Cu atoms and are thus preferably chelated. Due to this, the ^{65}Cu atoms preferentially remain in the tumour tissue, resulting in an increase of the $^{65}Cu/^{63}Cu$ isotope ratio in the tumour tissue and a corresponding decrease of the serum $^{65}Cu/^{63}Cu$ isotope ratio.[30]

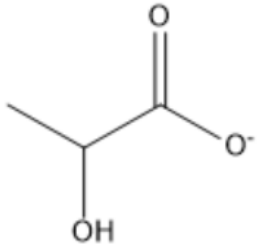

Figure 4 Structure of lactate.

In the future, the $^{65}Cu/^{63}Cu$ isotope ratio may be able to aid conventional diagnostic techniques when they are inconclusive. However, larger scale studies are still required to determine the threshold at which the $\delta^{65}Cu$ value indicates the presence of the disease.[30]

2.4 Cisplatin and carboplatin

Although this research focusses mainly on isotopic analysis of Pt in chemosensitive and chemoresistant cells and not on the clinical aspect, carboplatin and cisplatin are the source of the Pt in the cells and it is therefore relevant to provide details concerning these chemotherapeutic agents.

Carboplatin (cis-diammine-1,1-cyclobutene decarboxylate platinum [II]) is a chemotherapeutic agent based on Pt that was developed to try and decrease the negative effects of cisplatin (cis-diamminedichloroplatinum[II]),[32] which is one of the first and most-used metal-based chemotherapeutic drugs.[33] Figures 5a and 5b show the structure of these chemotherapeutic agents.

Figure 5a

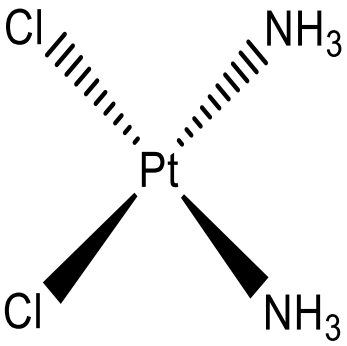

Figure 5b

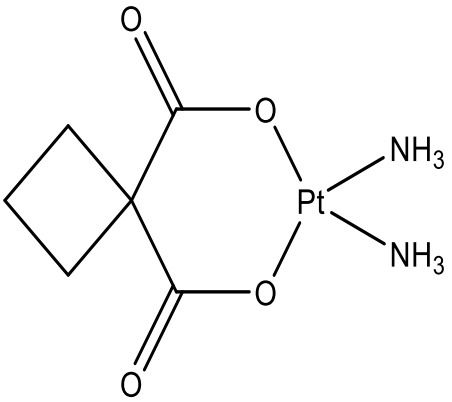

Figure 5a Structure of cisplatin and **Figure 5b** Structure of carboplatin.

Both cisplatin and carboplatin are especially effective against testicular and ovarian cancer. They are amongst the most commonly used chemotherapeutic drugs and have an identical range of action, carboplatin however exhibits lower neuro- and nephrotoxicity (toxicity to the nervous system and kidneys respectively) compared to cisplatin.[34]

Cisplatin is most likely transported into cancerous cells by CTR1, and once in the cell, cisplatin undergoes an activation step by chloro-ligand(s) replacement. The chloro-ligands are typically replaced by water molecules or small molecules containing sulfhydryl groups and this is a result of the lower intracellular Cl^- ion concentration (~4 mM) in the cytoplasm compared to the concentration in the extracellular matrix (~100 mM), promoting transformation to cationic hydrates, such as cis-$[Pt(NH_3)_2Cl(OH_2)]^+$ and cis-$[Pt(NH_3)_2(OH_2)_2]^{2+}$ (Figure 6) (Zhang, 2022). After a series of chemical reactions in the cytoplasm, Pt binds to DNA by forming crosslinks, which changes the structure of, and causes damage to, the DNA. The most nucleophilic DNA site is the N7 position of the amino acid guanine, which is exposed in the major groove and is preferentially platinated.[35] Platinum isotopic fractionation may occur during this stage due to the binding of Pt by the N ligand of guanine, which due to its higher electronegativity would favour ^{198}Pt-containing cisplatin compared to Pt bound by a S ligand, such as in cysteine, Ih would favour ^{194}Pt-containing cisplatin. This forms part of the theoretical basis of this investigation, but there is also potential for Pt isotopic fractionation to occur during processes related to the importation of the Pt drug to the cell, exportation of the Pt drug from the cell,

and the trapping of cisplatin by cellular metallothionein, a cysteine-rich, low molecular weight protein, which may contribute to cisplatin resistance, among others.[36]

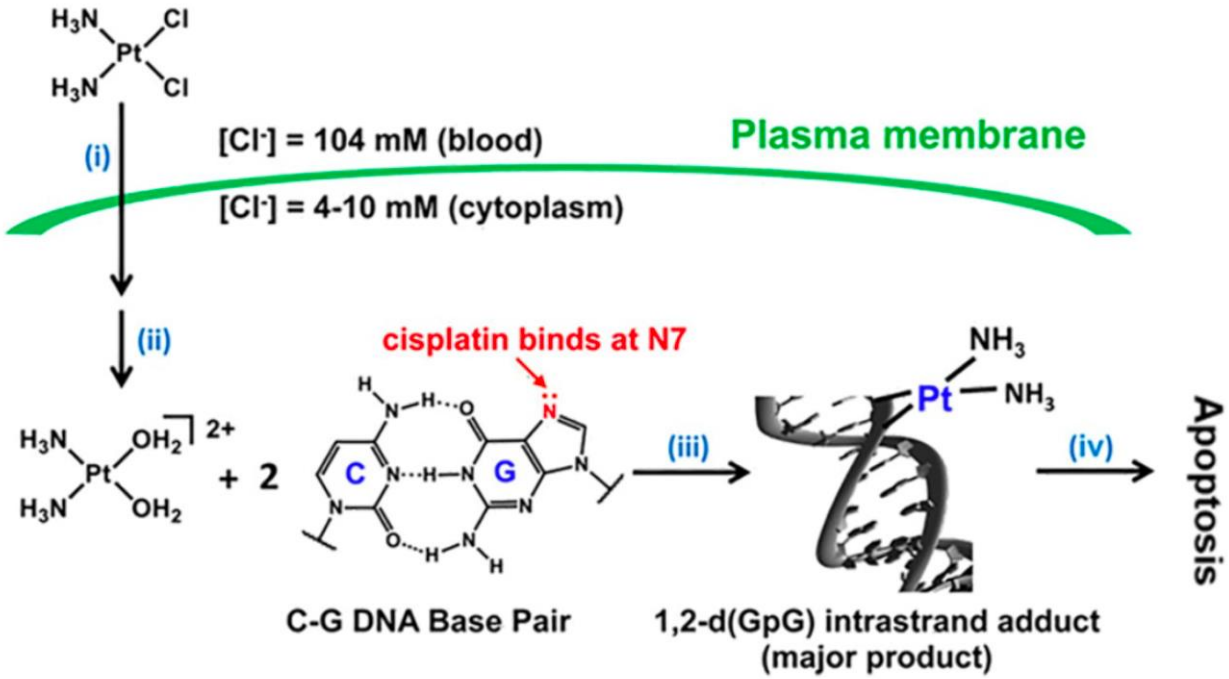

Figure 6 Cisplatin mechanism of action: (i) cellular uptake, (ii) aquation/activation, (iii) DNA platination, (iv) cellular processing leading to apoptosis (Zhang, 2022).

Di Pasqua et al. gave an overview of the chemistry of carboplatin.[37] Its most notable feature is the bidentate dicarboxylate chelate leaving ligand, which can also be seen in Figure 5b above. This ligand (cyclobutene-1,1-dicarboxylate) is responsible for lowered reactivity compared to cisplatin. Carboplatin binds to proteins, Human Serum Albumin for example, but once again this takes a longer time compared to cisplatin (only 40% of carboplatin is bound to proteins after 24 hours). After it passes through the blood, carboplatin most likely enters the cell through passive diffusion. While it was also suggested that the copper transporter CTR1 could be involved with the transport into the cell,[37] results from a study by Crider et al. hint that CTR1 probably does not facilitate entry of carboplatin in the cell in a therapeutic window,[38] in contrast to cisplatin, which most likely does enter cells by CTR1.

3. Research objectives:

This thesis project aims at the development of the methodology required to explore whether Pt isotopic fractionation occurs in response to the development of chemoresistance in ovarian cancer cell lines. It will also provide a first investigation of this topic by administering carboplatin and cisplatin to commercially available chemosensitive and cisplatin-resistant versions of the A2780 ovarian cancer cell line. Carboplatin was also selected as it is the most commonly employed chemotherapeutic drug against ovarian cancer and there is evidence of cross-resistance for carboplatin in A2780, meaning the cell line is resistant to both cisplatin and carboplatin.[39] Differences in the way Pt isotopes are fractionated in chemosensitive and cisplatin-resistant ovarian cancer may reveal mechanisms of Pt-based chemotherapeutic drug resistance and could, in the future, lead to the discovery of novel markers for chemoresistance.

4. Research method and Work Packages:

This research will be divided into four work packages (WPs):

WP1 Calibration of a chromatographic protocol for Pt isolation.

WP2 Development of a measurement protocol for accurate and precise determination of Pt isotope ratios by MC-ICP-MS.

WP3 Cell culturing and Pt-drug exposure.

WP4 Pt quantification and Pt isotopic analysis of cells and growth medium.

This research project poses several analytical challenges and will also involve (i) calibrating chromatographic procedures intended to isolate Pt from different sample types prior to isotopic analysis, (ii) identifying suitable biological reference materials to dope with Pt and use to validate Pt isotope ratio measurements, and (iii) adapting the measurement protocol as to determine Pt isotopic compositions at low (<20 ng g^{-1}) Pt concentrations.

Due to the low abundance of Pt in nature and limited biological role compared to essential mineral elements, Pt contamination is anticipated to be minimal and confounding processes influencing isotopic fractionation minimized, thus presenting a unique research opportunity to track the redistribution of Pt isotopes associated with chemoresistance in a closed system.

4.1 Work Package 1: Calibration of a chromatographic protocol for Pt isolation.

To avoid matrix effects during Pt isotope ratio measurement by MC-ICP-MS, Pt must be separated from other components of the sample matrix. There are chromatographic methods for Pt isolation available from literature, but many of the existing methods are lengthy and require many different reagents as they were calibrated to remove many of the heavy elements found in meteorites.[22] The matrix of biological samples is much less complex than meteorites, so existing methods will be simplified and optimized for this new matrix type, which will also reduce contamination. Preliminary testing with a synthetic sample (composition according to Table 2) performed for this thesis (Figure 7) indicated that chromatographic procedures described in literature can be significantly shortened (by 2/3) for biological matrices. The simplified protocol (Figure 8) will be validated using biological reference materials doped with Pt of known isotopic composition. If the chromatographic method calibrated for this thesis is performing adequately, the Pt isotopic composition of the Pt solution used for doping should be the same before and after chromatography.

Table 2 Composition of the synthetic sample used for preliminary testing of a chromatographic protocol for Pt isolation.

Element	Loaded onto column (µg)
Na	0.998
Mg	0.997
K	0.994
Ca	1.010
Fe	0.507
Cu	0.203
Zn	0.503
Pt	0.093

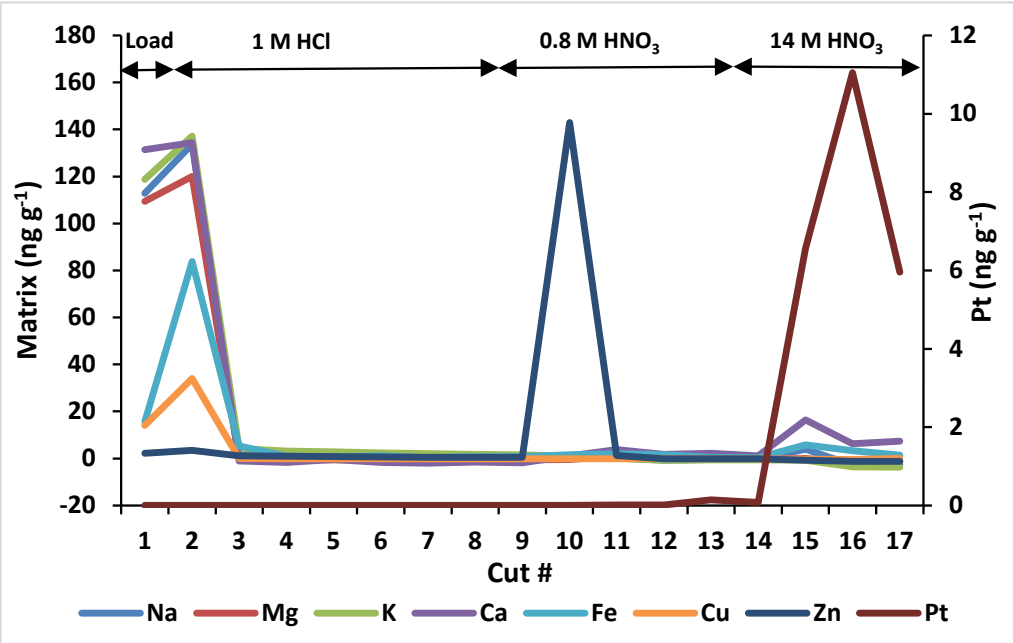

Figure 7 Elution profile of first chromatography test showing that reagent volumes can be further reduced due to matrix elements coming off of the column earlier. A different axis was used for Pt because the concentration of Pt was lower than the concentration of the other elements. Cut #1 (load) = 1 mL of 1 M HCl; Cut #2-9 = 6.65 mL of 1 M HCl each; Cut #10-14 = 4 mL of 0.8 M HNO_3 each; Cut 15-17 = 4 mL of 14 M HNO_3 each.

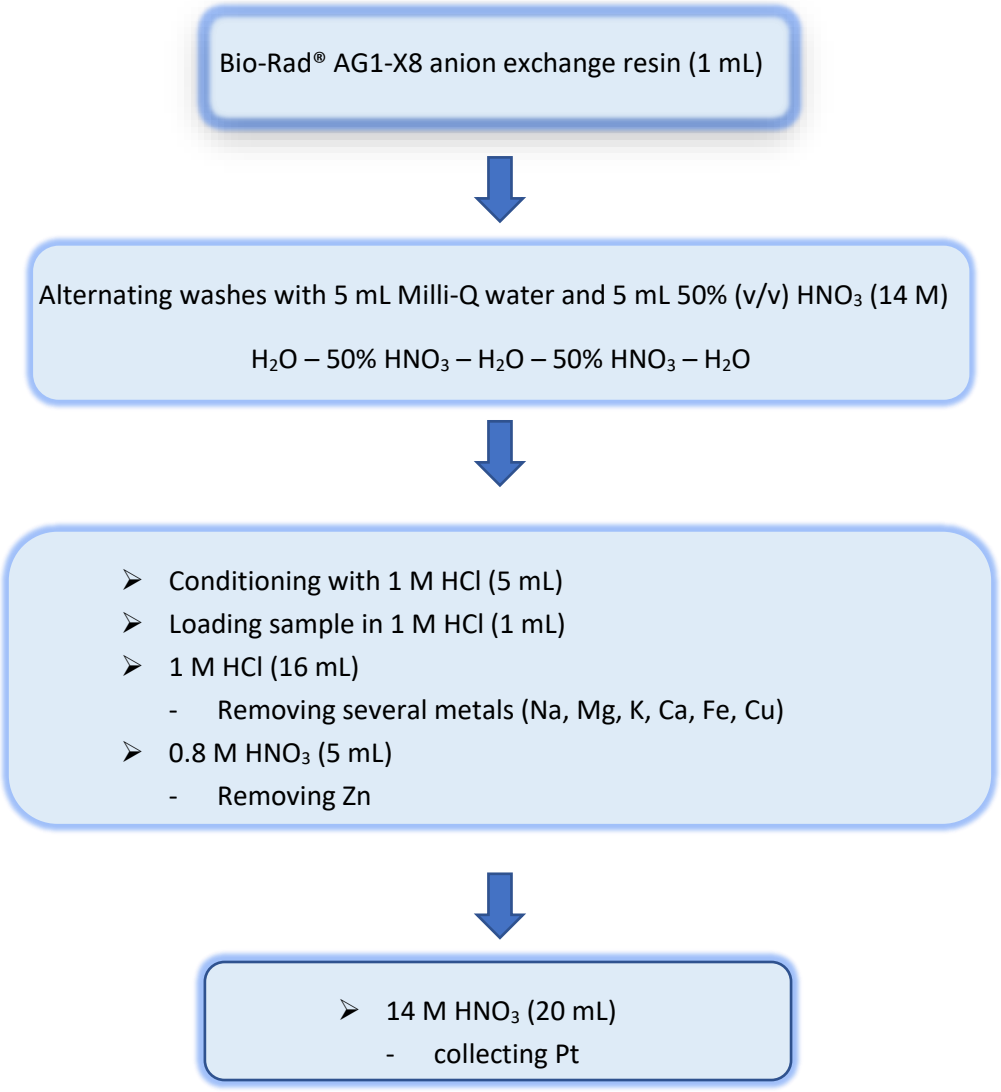

Figure 8 Simplified chromatographic protocol for isolation of Pt based on preliminary testing.

4.2 Work Package 2: Development of a measurement protocol for accurate and precise determination of Pt isotope ratios by MC-ICP-MS.

There is risk for on-column Pt isotope fractionation, such that quantitative analyte recovery is required to avoid this phenomenon from affecting the final results. As a result, Pt quantification will be performed before and after isolation.[40, 41] Platinum concentrations will be determined using an Agilent 8800 ICP-MS system (Agilent Technologies). The concentration of the essential mineral elements (Na, Mg, K, Ca, Fe, Cu, Zn) will also be determined with this system, with NH_3 and He as reaction/collision gasses to avoid interferences. Quantitative data will be obtained using external calibration with Ga (Inorganic Ventures, VA, USA) as an internal standard to correct for potential matrix effects and signal instabilities.

Platinum isotope ratios will be determined using a Neptune *Plus* MC-ICP-MS unit (ThermoScientific, Bremen, Germany). The advantage of using this instrumentation is that it is equipped with 10^{13} Ω Faraday cup resistors, which will improve the ability to perform precise Pt isotope ratio measurements at low concentrations.[42] Analytical precision is among other things limited by thermal noise, also reffered to as Johnson – Nyquist noise. However, when the resistor value is increased, the sensitivity will increase linearly, whilst the relative noise increases by the square root of the resistor value only.[43] So increasing the resistor value improves the signal-to-noise ratio and also improves the repeatability of isotope ratios derived from lower ion beam intensities.[42] A comparison of the Pt isotope ratio measurement performance with 10^{11} and 10^{13} Ω feedback resistors will be conducted.

Compared to essential mineral elements, the magnitude of Pt isotope ratio variations are expected to be small due to the small relative difference in mass between isotopes of Pt. External correction using a Pt isotopic standard measured in a sample-standard bracketing (SSB) sequence combined with internal normalization using Ir as an internal standard will be investigated as an approach to correct for instrumental mass bias.[44] Iridium is ideal for this task due to its occurrence in extremely low quantities in biological materials and it being close in mass to the isotopes of Pt, while suffering no spectral overlap.[45] To the best of our knowledge, this will be the first instance in which Pt isotope ratio data will be corrected for mass bias using Ir as an internal standard. This method offers several advantages over the Pt double-spike mass bias correction that is typically used to correct instrumental mass bias due to being simpler, quicker, and cheaper to implement. The Pt isotope ratio variations will be reported in terms of δ^{198}Pt which is the deviation of the ^{198}Pt/^{194}Pt ratio from the sample to the same ratio in a standard. For this thesis, the Pt isotope standard IRMM-010 will be used. This method of reporting and standard are also used by Creech et al.[20] and the values are calculated according to Equation 2.

$$\delta^{198}\mathrm{Pt} = \frac{\left(\frac{^{198}Pt}{^{194}Pt}\right)_{sample} - \left(\frac{^{198}Pt}{^{194}Pt}\right)_{IRMM-010}}{\left(\frac{^{198}Pt}{^{194}Pt}\right)_{IRMM-010}} \cdot 1000(‰) \qquad \text{[Equation 2]}$$

4.3 Work Package 3: Cell culturing and Pt-drug exposure.

Commercially available cell lines will be used during this project. The chemosensitive ovarian carcinoma cell line, A2780, and its cisplatin-resistant subline A2780cis were selected because the resistance does not need to be trained, only maintained, saving a significant amount of time.

The cytotoxicity of carboplatin and cisplatin in the A2780 and A2780cis cell lines will be tested using the CellTiter-Glo® Luminescent Cell Viability Assay, which is a method for determining the number of viable cells in a culture based on quantitation of the amount of ATP present, as this is an indicator of metabolically active cells. This will provide the IC_{50}, or concentration of the drug at which 50% of the cells are inhibited by the drug. The cell treatment and doses used in the exposure experiments will predominantly follow those described by Schoeberl et al. and cells will be exposed to a concentration that is approximately 2 times the IC_{50} of the drugs for A2780cis for 6 hours.[18]

4.4 Work Package 4: Pt quantification and Pt isotopic analysis of cells and growth medium.

To minimize the potential of contamination, all sample preparation procedures will be performed in a class-10 clean room laboratory (PicoTrace, Göttingen, Germany). Ultra-pure water will be prepared using a Milli-Q water purification system (Merck Millipore, Molsheim, France). Pro-analysis grade HNO_3 (Chem-Lab, Zedelgem, Belgium) and HCl (Fisher Chemicals, Loughborough, UK) will be further purified by subboiling distillation in a Savillex DST-4000 acid purification system (Savillex Corporation, Eden Prairie, MN, USA).

Samples will be digested on a hotplate at 120 °C in 5 mL of concentrated HNO_3 and 1 mL of 30% (w/w) H_2O_2 per 0.2 g of material prior to elemental and isotopic analysis. Platinum concentrations and isotope ratios will be measured in both chemosensitive and chemoresistant ovarian cancer cell lines and growth medium using procedures developed through WP1 to WP3.

4.5 Tentative timetable

Table 3 shows a tentative timeline regarding the completion of the work packages. Experimental work includes studying literature as well. Milestones signify when a work package is expected to be completed. Deliverable 4A is the written version of the thesis and deliverable 4B is the final presentation.

Table 3 Gantt chart showing the tentative schedule of the work packages.

Work Package	WP1	WP2	WP3	WP4
Title	Chromatography	Validation	Cell culturing	Isotopic analysis
February				
March				
April				
May	M1			
June				
July				
August		M2		
September			M3	
October				
November				
December				M4
January				D4A/D4B
Legend	Experimental work			
	Milestone	M		
	Deliverable	D		

4.6 Risk assessment and mitigation

There are both experimental and analytical risks associated with this research. The risk of instrumentation issues compromising the ability to complete this research is minimal due to mitigation by (1) a full-time technician being employed to maintain normal functioning of the instrumentation and (2) multiple instruments being available at A&MS that may be employed for this research. Experimental risks are mostly related to not being able to resolve the very small amount of Pt isotope fractionation that is expected between chemosensitive and chemoresistant cells. Improved analytical precision will mitigate this risk, and to that end, the external correction in combination with Ir as an internal standard will be employed. If no changes in Pt isotopic fractionation can be resolved even with improved measurement precision, the level of resistance to Pt-based chemotherapeutic drugs can be increased in the cell line over time through additional cisplatin exposure, which may improve the likelihood of inducing a Pt isotopic effect. Different ovarian cancer cell lines can also be studied, such as SKOV-3 and OVCAR-3.

5. Research Project:

In the following parts, all experiments and results will be reported and discussed. This also includes the results of the preliminary research. To keep a clear overview, this part is divided in different sections: materials and reagents, samples, preparation and experimental work. The experimental work was based on the proposed work packages of the research plan. It is however worth noting that certain observations or limitations during the experimental work led to a slight deviation of said work packages. Since more lab time was available, the experiments were more detailed compared to the general outline of these work packages as well.

Cell samples were limited, consequently the measurement procedure had to function properly before working with these limited samples to not waste them. Testing of the measurement protocol, including chromatography and contamination tests took longer than expected. Therefore the focus of this thesis was shifted to getting the measurement protocol to work properly (work package 1 and 2) instead of measuring the cell samples (work package 4). Consequently, the fourth work package proposed in the research plan was not prioritized during the thesis.

6. Materials & reagents

Ultra-pure water was prepared using a Milli-Q water purification system (Merck Millipore, Molsheim, France). Pro-analysis grade HNO_3 (Chem-Lab, Zedelgem, Belgium) and HCl (Fisher Chemicals, Loughborough, UK) was further purified by subboiling distillation in a Savillex DST-4000 acid purification system (Savillex Corporation, Eden Prairie, MN, USA). Sample preparation procedures were performed in a class-10 clean room laboratory (PicoTrace, Göttingen, Germany). Hydrogen peroxide (H_2O_2) was also used for post-column sample treatment and sample digestion.

7. Samples

- IRMM-010

IRMM-010 is the standard reference material with a known Pt isotopic composition that was used during this thesis. The δ-values were calculated relative to this standard, just like it has been done before in previous Pt isotopic analysis research.[20, 22]

- Platinum-α

Platinum-α (Pt-α) was used as an inhouse Pt standard to prepare the synthetic samples and to test the measurement protocol. It is the inhouse Pt standard that was used in previous research by Poole et al.[22] and since it has a determined δ-value relative to IRMM-010, the proper functioning of the measurement protocol can be confirmed if results are comparable to the results reported by Poole et al.[22]

- Reference material Seronorm Serum L-1

Seronorm™ Trace Elements Serum L-1 was used as a reference material for method validation of element quantification.

- Cell samples

As mentioned in the research plan the ovarian cancer cells, A2780 cells, and its cisplatin resistant variant, A2780cis cells, were used during this thesis. Both cell lines were either treated with cisplatin or not and the media in which they were cultured was collected as well. For this thesis the most relevant cell samples were two A2780 cell samples treated with cisplatin and two A2780cis cell samples treated with cisplatin. Treating the samples involved exposing them to 10 µM cisplatin for 6 hours.

Whenever the concentration of the samples was checked, on the 8800 or the Xseries II instruments, Ga from a 1000 mg/L standard solution (Inorganic Ventures, VA, USA) was added to the samples as an internal standard with a concentration of 10 µg/L. For measurements on the Neptune instrument, platinum samples were diluted in 0.5 M HCl to improve wash out time. For all other measurements the samples were diluted in 2% (V/V) (15.6 M) HNO_3 in Milli-Q water.

8. Preparation

8.1 Titration

The concentrated hydrochloric acid (HCl) and nitric acid (HNO_3) were both titrated against 1 M NaOH to check the concentration using phenolphthalein as an indicator. The titration test confirmed the molarities of the concentrated acids: 15.6 M and 10.6 M for concentrated HNO_3 and concentrated HCl respectively. Knowing the concentration of the concentrated acids was necessary since these acids were used to prepare the acidic solutions that were used during this thesis.

8.2 Calibration standards

In order to determine the concentration of elements in samples, a calibration curve has to be prepared. The composition of the calibration standards that were used during this thesis are displayed in Table 4.

Table 4 The calibration standards used during this thesis.

Cal. Std #	Na (µg/L)	Mg (µg/L)	K (µg/L)	Ca (µg/L)	Fe (µg/L)	Cu (µg/L)	Zn (µg/L)	Pt (µg/L)	Ga (µg/L)
0	0.0	0.0	0.0	0.0	0.0	0.0	0.0	0.0	10.0
1	1.0	1.0	1.0	1.0	0.5	0.2	0.5	0.1	10.0
2	5.0	5.1	5.1	5.2	2.6	1.0	2.6	0.5	10.0
3	10.1	10.2	10.2	10.3	5.2	2.1	5.1	1.0	10.0
4	25.1	25.5	25.4	25.9	13.0	5.2	12.8	2.4	10.0
5	50.3	51.0	50.8	51.7	26.0	10.5	25.7	4.9	10.0

9. Results and discussion

9.1 Preliminary research

During the preliminary research, the focus was on developing the procedure for chromatographic isolation of Pt. As mentioned in the research plan, the procedure was mainly based on the method reported by Creech et al.[20] The amounts of the elements loaded onto the column for the first test are found in Table 5. Table 6 shows the procedure of the first chromatography test.

Table 5 Composition of the synthetic sample used for preliminary testing of Pt chromatography.

Element	Loaded onto column (µg)
Na	0.988
Mg	0.997
K	0.994
Ca	1.010
Fe	0.507
Cu	0.203
Zn	0.503
Pt	0.093

Table 6 Chromatographic procedure for Pt isolation out of a biological matrix based on Creech et al.[20]

Resin: Bio-Rad AG1-X8, 200 -400 mesh, chloride form, 1 mL		
Step	Resin volume	Eluent
Cleaning	5 mL	H_2O
	5 mL	7.8 M HNO_3
	5 mL	H_2O
	5 mL	7.8 M HNO_3
	5 mL	H_2O
Conditioning resin	5 mL	1 M HCl
Loading sample (cut 1)	1 mL	1 M HCl
Eluting Na, Mg, K, Ca, Fe, Cu (cut 2-9)	53.20 mL (total) 6.65 mL (each cut)	1 M HCl
Eluting Zn (cut 10-14)	20 mL (total) 4 mL (each cut)	0.8 M HNO_3
Eluting Pt (cut 15-17)	12 mL (total) 4 mL (each cut)	15.6 M HNO_3

Results of this first test can be seen in Figure 9. Most of the elements eluted from the column earlier than expected, indicating that the procedure could be shortened. Platinum, for which the concentration is projected on the right y-axis, was also not fully eluted from the column. This suggests that more concentrated HNO_3 is needed to completely elute the Pt. During this first test, and all the following chromatography tests, the resin changed from a yellow color to a bright red color when using concentrated HNO_3. This observation was not mentioned in literature[20, 22] and could possibly affect the results.

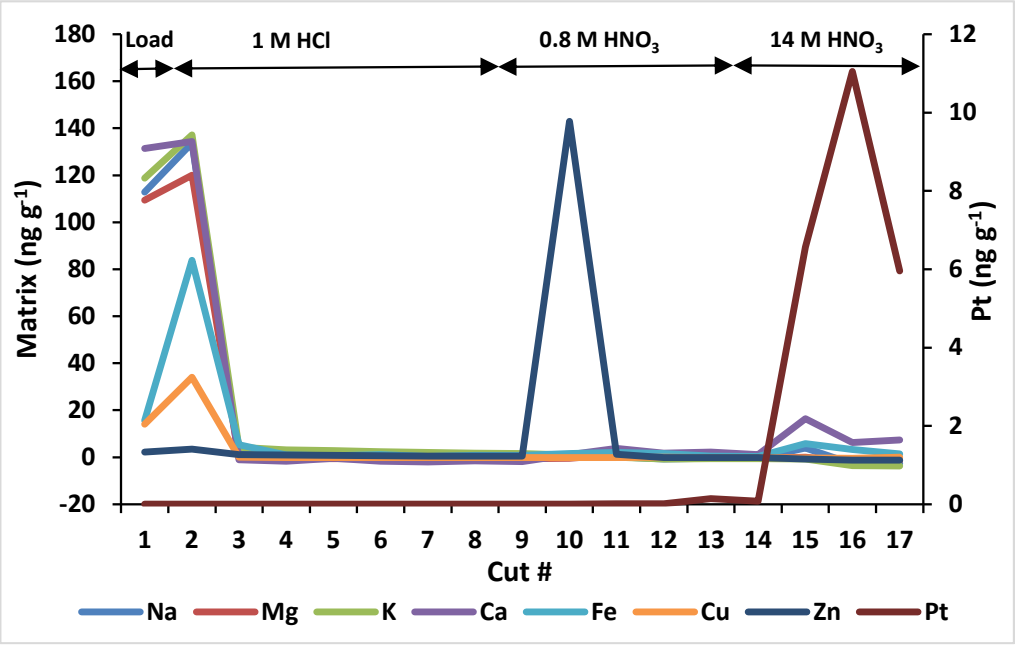

Figure 9 Result of the first chromatographic procedure showing the concentration of elements in the synthetic sample in each cut. All concentrations are projected on the left y-axis, except that of Pt which is projected on the right y-axis.

Based on these results, a second test was carried out, which involved using smaller volumes of acid to elute the matrix elements. The same synthetic sample (Table 5) was loaded onto the column. The procedure for this test is described in Table 7.

Table 7 Simplified chromatographic procedure for Pt isolation out of a biological matrix based on preliminary research.

Resin: Bio-Rad AG1-X8, 200 -400 mesh, chloride form, 1 mL		
Step	Resin volumes	Eluent
Cleaning	5 mL	H_2O
	5 mL	7.8 M HNO_3
	5 mL	H_2O
	5 mL	7.8 M HNO_3
	5 mL	H_2O
Conditioning resin	5 mL	1 M HCl
Loading sample (cut 1)	1 mL	1 M HCl
Eluting Na, Mg, K, Ca, Fe, Cu (cut 2-9)	16 mL (total) 4 mL (each cut)	1 M HCl
Eluting Zn (cut 10-14)	5 mL (total) 1 mL (each cut)	0.8 M HNO_3
Eluting Pt (cut 15-19)	20 mL (total) 4 mL (each cut)	15.6 M HNO_3

Instead of using 53.20 mL of 1 M HCl in the first eluting step, only 16 mL of 1 M HCl was used. The volume of 0.8 M HNO_3 was also reduced from 20 mL to 5 mL. To make sure that all the Pt was eluted from the column, 20 mL of 15.6 M HNO_3 was used in the final step.

The results of this second test are displayed in Figure 10. This time, negligible Pt was present in the final cut, indicating quantitative recovery from the column. The other elements were also eluted, but Fe took longer to attenuate, and could possibly be a cause of contamination. Future tests took this observation into account.

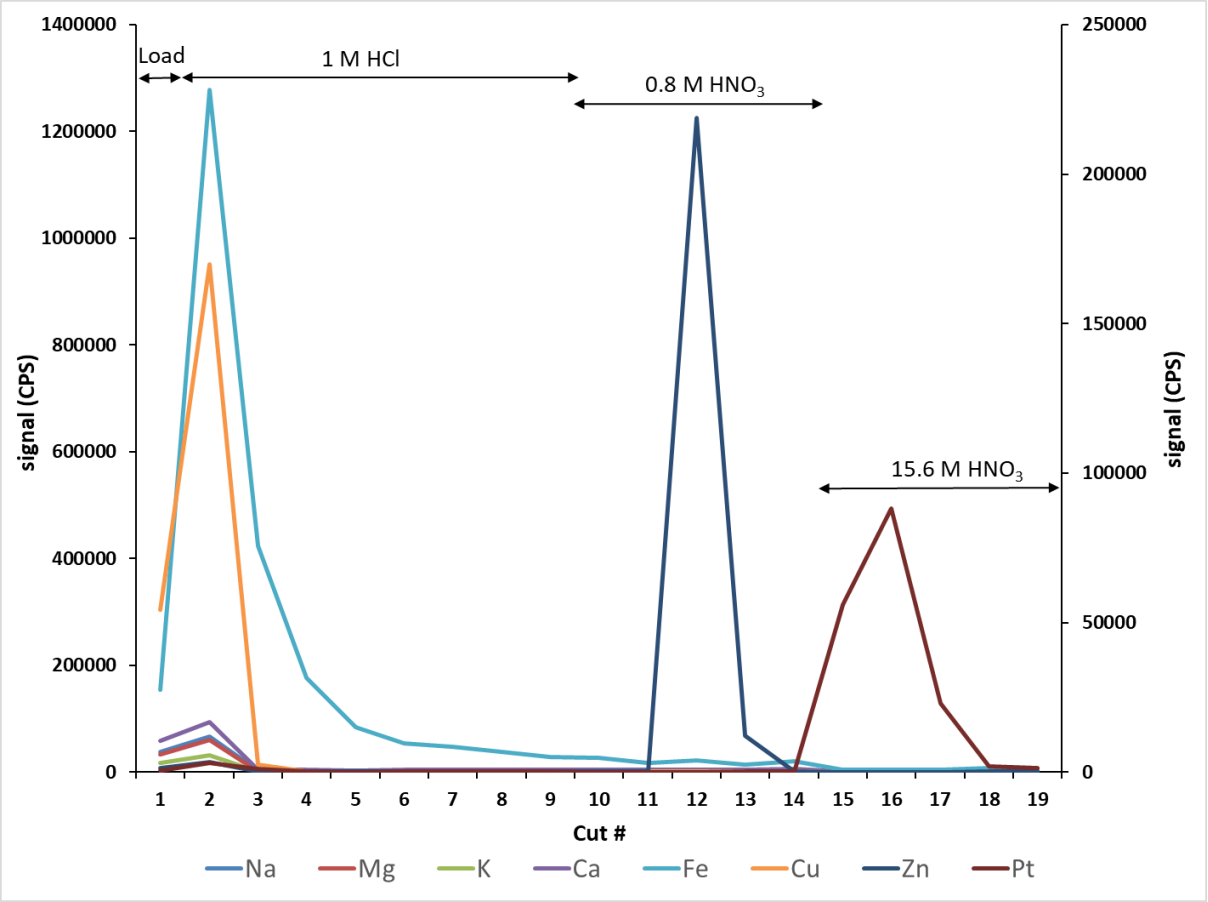

Figure 10 Result of the second, simplified chromatographic procedure. The signal for Fe, Cu, Zn and Pt is projected on the right y-axis. The signal for the remaining matrix elements is projected on the left y-axis.

This optimized chromatographic procedure for Pt isolation was used for subsequent tests involving samples with complex biological matrices. Zinc also appears to elute relatively free from interferences, indicating that the feasibility of using this procedure for Zn isotopic analysis could be explored.

9.2 Testing of the chromatographic procedure

The proposed chromatographic procedure had to be tested before applying it to actual cell samples. A synthetic "cell" solution with the approximate composition of a digest of A2780 cells treated with cisplatin was prepared. This synthetic cell solution could then already indicate whether the chromatographic procedure functioned properly at the concentration levels expected in the cell samples.

Table 8 Composition of the synthetic "cell" solution used for testing the chromatographic procedure for Pt isolation out of a biological matrix.

Element	Loaded onto column (µg)
Na	265.130
Mg	14.719
K	106.973
Ca	3.693
Fe	0.374
Cu	0.054
Zn	1.287
Pt	0.098

Due to a high Pt blank observed for the 8800 ICP-MS/MS instrument, the measurement could not confirm whether Pt already elutes during the use of 1 M HCl and 0.8 M HNO_3. A measurement using a different instrument, a ThermoScientific Xseries II quadrupole-based ICP-MS instrument, did however show that the Pt amount in the 15.6 M HNO_3 collected fraction corresponded to the amount of Pt loaded onto the column, showing that the Pt is most likely fully eluted during this phase. Due to the inconclusive results, the efficiency of the chromatographic procedure was tested once more, this time only using the Xseries II ICP-MS instrument.

9.3 Xseries II ICP-MS measurements

The efficiency of the chromatographic procedure was examined by measuring the Pt concentrations in the three different fractions, 1 M HCl, 0.8 M HNO_3 and 15.6 M HNO_3, that were collected. Instrument settings for the Xseries II instrument can be found in Table 9.

Table 9 XSeries II ICP-MS operating conditions.

Instrument settings	
Sample uptake rate	0.5 mL min^{-1}
cool gas flow rate	13.0 L Ar min^{-1}
Auxiliary gas flow rate	0.74 L Ar min^{-1}
Nebulizer gas flow rate	0.79-0.84 L Ar min^{-1}
Sample and skimmer cone	Nickel, Xt-type
RF power	1200 W
Data acquisition parameters	
Integration time	0.030 s
Blocks	3
Cycles/block	100
Total data acquisition time	9 s per nuclide
Total measurement time	9 s per nuclide

Since the synthetic sample was prepared with known concentrations, the sum of the masses of Pt in the different fractions should be equal to the total mass that was loaded onto the column. The Pt recovery in the final fraction should be as high as possible. Therefore the first fractions should have a concentration of Pt as low as possible, which is dependent on how effective the separation procedure is. Table 10 shows the expected concentration and the calculated concentration in the final collected fraction (15.6 M HNO_3). The Fe and Ca concentrations were impossible to determine, because all the calibration standard solutions provided the same signal. As a result, the instrument was not capable of producing a calibration curve and concentrations could therefore not be determined. Potassium could not be measured on the XseriesII instrument due to spectral overlap with Ar and the lack of effective reaction/collision gasses.

Table 10 Calculated and measured concentration in the final fraction of the chromatographic procedure.

Fraction which eluted Pt	Na	Mg	Ca	Fe	Cu	Zn	Pt
Measured concentration (µg/L)	< DL	0.080	/	/	< DL	0.078	1.13
Expected concentration (µg/L)							0.98

In the first two collected fractions (1 M HCl and 0.8 M HNO_3), the Pt concentrations were below the detection limit, suggesting that these fractions contained almost no Pt. This was confirmed by the measured concentration in the final fraction, seen in Table 10. Since this measured concentration was close to the concentration that was expected based on the amount of Pt loaded onto the column, almost all the Pt was eluted in this fraction. The difference between the measured concentration and the expected concentration based on how much Pt we loaded onto the column was potentially due to a combination of human errors that occurred for example during pipetting and a high/fluctuating Pt background signal. These results suggested that quantitative Pt recovery from the column was achieved.

Table 10 also shows that the column chromatography procedure is capable of separating the matrix elements from Pt. Both Na and Cu were present in a concentration below the detection limit. Magnesium and Zn were present in the final fraction, but the Mg/Pt and Zn/Pt ratios were low. Results reported later in this thesis also indicated that the concentration ratios at this level did not have an influence on the determination of the δ-value. Based on these results, the chromatographic procedure seemed to function properly at the concentration levels that were expected to be present in the A2780(cis) cell samples.

9.4 Neptune measurements (isotopic analysis)

The next step in this thesis was developing a measurement protocol to determine Pt isotope ratios using MC-ICP-MS. The following sections will all provide results for various isotope ratio measurements. The instrument settings for the Neptune MC-ICP-MS instrument can be found in Table 11.

Table 11 Neptune MC-ICP-MS operating conditions.

Instrument settings	
Forward power	1200 W
Plasma gas flow rate	15 L Ar min^{-1}
Auxiliary gas flow rate	0.70 to 0.95 L Ar min^{-1}
Nebulizer gas flow rate	~ 1 L Ar min^{-1}
Sample cone	Nickel, Jet-type: 1.1 mm orifice diameter
Skimmer cone	Nickel, X-type: 0.8 mm orifice diameter
Sample uptake rate	0.1 mL min^{-1}
Mass resolution mode	Low
Data acquisition parameters	
Faraday cup configuration/amplifier	L3 (^{191}Ir)/10^{11} Ω, L1 (^{193}Ir)/10^{11} Ω, C (^{194}Pt)/10^{13} Ω, H1 (^{195}Pt)/10^{13} Ω, H2 (^{196}Pt)/10^{13} Ω, H3 (^{198}Pt)/10^{13} Ω
Sensitivity	0.33 V for ^{195}Pt at 10 ng mL^{-1} (ppb)
Signal integration time	4 s
No. of integrations, blocks, cycles/block	3 / 1 / 50
Blank signal (0.5 M HCl)	0.003 V for ^{195}Pt

The instrument and measurement protocol was tuned by measuring and determining the δ^{198}Pt-value for both IRMM-010 and Pt-α. The δ^{198}Pt-values, from now simply referred to as δ-values, were calculated according to the following equation:

$$\delta^{198}\mathrm{Pt} = \frac{\left(\frac{^{198}Pt}{^{194}Pt}\right)_{Pt-\alpha} - \left(\frac{^{198}Pt}{^{194}Pt}\right)_{IRMM-010}}{\left(\frac{^{198}Pt}{^{194}Pt}\right)_{IRMM-010}} \cdot 1000\ (‰) \qquad \text{[Equation 3]}$$

IRMM-010 is the standard used during this thesis and a δ-value for Pt-α relative to IRMM-010 is available in literature. If the measurement procedure functions properly, the δ–value for IRMM-010 should be zero since it is calculated relative to itself and the δ-value for Pt-α should be close to -0.07 ‰.[22]

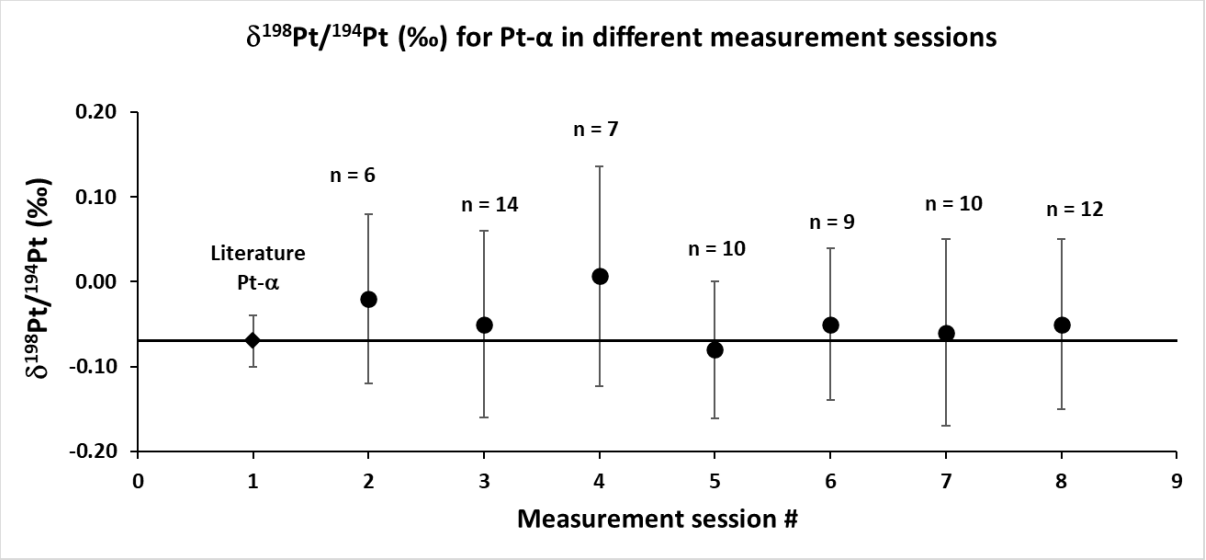

Pt-$\alpha_{IRMM\text{-}010}$ = -0.07 ± 0.03 ‰, Poole et al.[22]

Figure 11 Determined δ-values for Pt-α relative to IRMM-010 in different measurement sessions compared to the literature value (-0.07 ± 0.03 ‰). The number of measurements in one session is represented by n. The error bars represent 2 * standard deviation.

Table 12 δ-values determined for IRMM-010, cisplatin and Pt-α relative to IRMM-010. n represents the number of measurements performed.

Measurement session	Mean (‰)	2 * standard deviation	n
IRMM-010	0.02	0.12	3
1 (literature value)	-0.07	0.03	
2	-0.02	0.10	6
3	-0.05	0.11	14
4	0.01	0.13	7
5	-0.06	0.08	10
6	-0.05	0.09	9
7	-0.06	0.11	10
8	-0.05	0.10	12
Cisplatin	0.01	0.08	3

According to the results shown in Figure 11 and Table 12, the δ-value determined for IRMM-010 relative to IRMM-010 was around 0.00 ‰. The δ-value determined for Pt-α relative to IRMM-010 using the Neptune was close to the literature value[22], showing that the measurements performed in this thesis provided reliable results, although the precision was worse compared to previous studies. The low precision was likely related to the low Pt concentration in the samples (10 µg/L) and the use of sample-standard bracketing as a correction procedure, instead of double spike correction. The δ-value for Pt in cisplatin was also determined and is included in Table 12. This cisplatin was used to treat the cells and was therefore the source of Pt in the actual cell samples. To determine if resistance of ovarian cancer cells to cisplatin has an influence on Pt isotope fractionation, the δ-values for Pt in the A2780 and A2780cis samples treated with cisplatin can be compared to one another and to this determined value (0.01 ± 0.08 ‰).

9.4.1 SSB vs. C-SSBIN tests

Sample-standard bracketing combined with internal normalization was tested as a possible method for correction of the bias introduced by instrumental mass discrimination. In sample-standard bracketing, a sample is measured in-between two measurements of the standard, IRMM-010 in this case. The IRMM-010 $^{198}Pt/^{194}Pt$ ratio used to calculate the δ-value for the sample is the average of the $^{198}Pt/^{194}Pt$ ratios obtained in the two bracketing standard measurements. Using this average value corrects for drift of the signal over time. This procedure can however not fully correct for temporal drifts in instrumental mass discrimination, but this problem can be addressed by using another element as an internal standard.[46] Iridium was evaluated as an internal standard with a concentration of 100 µg/L in all samples. The Ir was measured at this concentration because the instrument can handle this high concentration and measuring at a higher concentration leads to better statistics. To the best of our knowledge this is the first time that Ir was used as an internal standard in the context of Pt isotopic analysis. Iridium was chosen because the two isotopes, ^{191}Ir and ^{193}Ir, are close in mass to the isotopes of Pt. There is no spectral overlap and Ir was not expected to be in the samples, which makes it a good internal standard.

These results for the δ-values were obtained through the combination of internal correction (with Ir) by means of the revised Russell's law and external correction in a sample-standard bracketing approach.[44] The same approach was also used in previous studies by Costas-Rodríguez et al.[47, 48] In this model, the corrected isotope ratio of Pt in a sample is calculated according to equation 4.

$$R_{Pt,corrected} = r_{Pt,sample} * \frac{\frac{m_2}{m_1}}{e^a * \left(r_{Ir,sample}\right)^b} \qquad \text{[Equation 4]}$$

In this equation m_2 is the mass of the heavy isotope, or ^{198}Pt in this case, m_1 is the mass of the light isotope, or ^{194}Pt in this case and r is the experimentally measured isotope ratio.

The parameters a and b refer to the intercept and slope of the best fitting linear curve in the graph of $\ln(^{198}Pt/^{194}Pt)$ versus $\ln(^{193}Ir/^{191}Ir)$. These ratios are measured in the bracketing standards. The slope and intercept are determined by linear regression analysis.

After correcting the Pt isotope ratios, the δ-values were calculated in a sample-standard bracketing approach using equation 3 and the corrected Pt isotope ratios. Results are found in Figure 12 and Table 13.

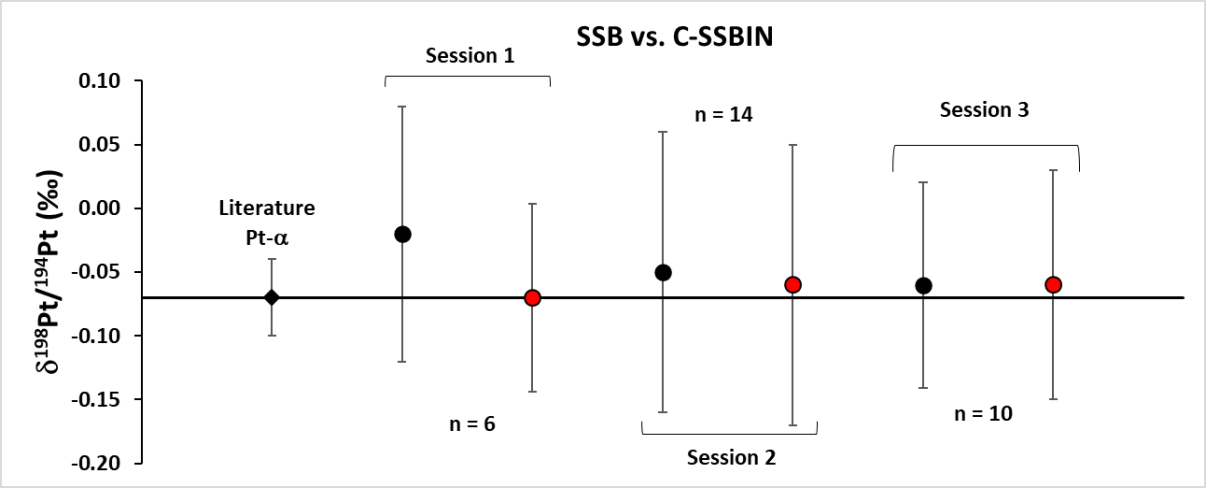

Pt-$\alpha_{IRMM-010}$ = -0.07 ± 0.03 ‰, Poole et al.[22]

Figure 12 Determined δ–values for Pt-α relative to IRMM-010 using sample-standard bracketing (SSB) as a correction procedure (black data points) or using a combination of – sample-standard bracketing with internal normalization (C-SSBIN) with Ir as an internal standard as a correction procedure (red data points). The number of measurements in one session is represented by n. The error bars represent 2 * standard deviation.

Table 13 comparison of determining the δ-value for Pt-α using the SSB method as a correction procedure versus using the C-SSBIN method with Ir as internal standard as a correction procedure for three different sessions.

Session 1			
	Literature	SSB	C-SSBIN
Mean (‰)	-0.07	-0.02	-0.07
2 * standard deviation	0.03	0.10	0.07
n		6	6
Session 2			
	Literature	SSB	C-SSBIN
Mean (‰)	-0.07	-0.05	-0.06
2 * standard deviation	0.03	0.11	0.11
n		14	14
Session 3			
	Literature	SSB	C-SSBIN
Mean (‰)	-0.07	-0.06	-0.06
2 * standard deviation	0.03	0.08	0.09
n		10	10

In the first session, using Ir as an internal standard, improved both the accuracy and precision of the δ-value for Pt-α relative to IRMM-010. Proving that there was potential for this model to work. However, the following measurements, session 2 and session 3, could not reproduce the same results and therefore it was concluded that using Ir as an internal standard to correct Pt isotope ratios did not provide added value for measurements performed during this thesis. Consequently, regular sample-standard bracketing was used as the correction procedure for all measurements.

The first session provided promising results, whilst the second and third session could not reproduce these results. This is because ln(^{198}Pt/^{194}Pt) and ln(^{193}Ir/^{191}Ir) were highly correlated in the first session, but not in the following ones. The correlation coefficient and graphs for the three session are represented in Figures 13.a,b and c.

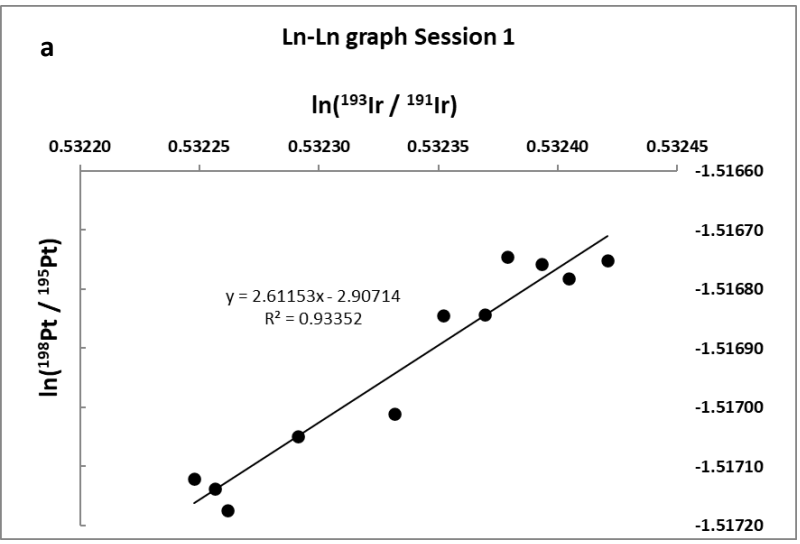

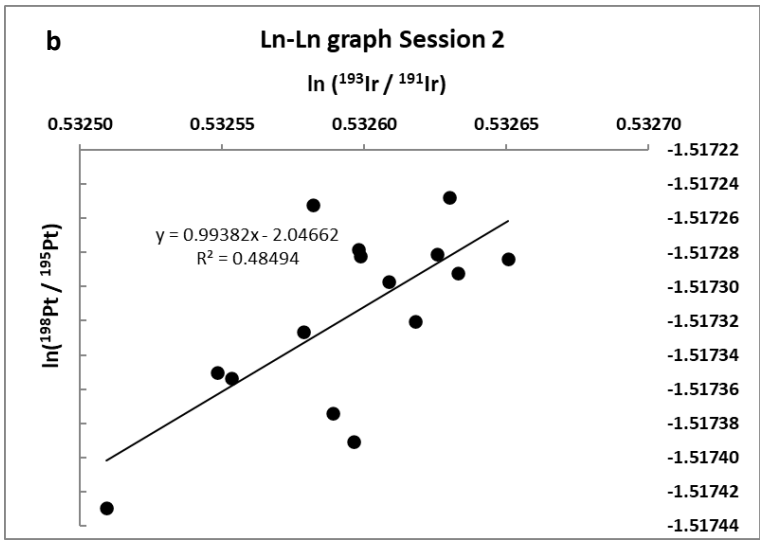

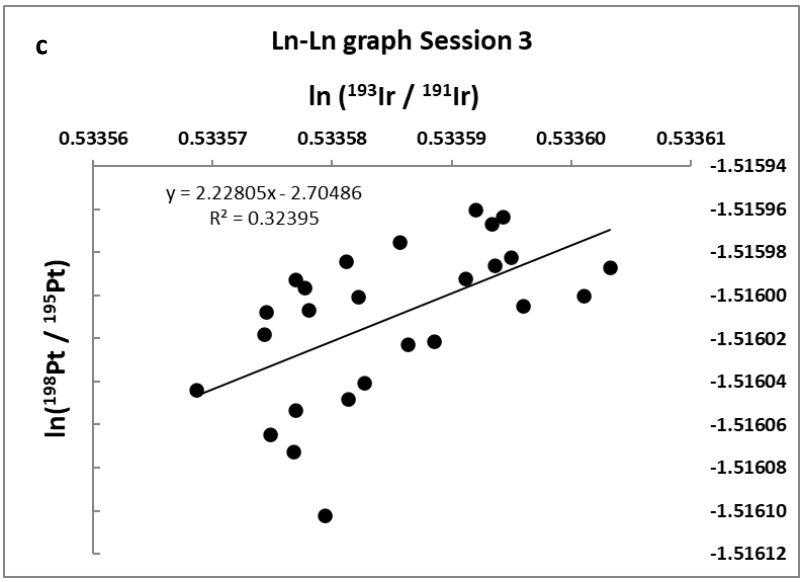

Figure 13a,13b and 13c Ln-Ln graph for the different measurement sessions, including the correlation coefficient and equation for the best fitting linear curve.

9.4.2 Contamination tests

The samples should be relatively free of contaminants after the chromatographic procedure. However, contamination could be introduced during experimental work and this contamination might have an influence on the results. According to the chromatographic tests, Fe could potentially be present in the Pt fraction. Solutions were prepared which had a Na, Mg, K, Ca or Fe concentration of 40 µg/L and a Pt concentration of 10 µg/L (4/1 concentration ratio) to determine whether the δ-value for Pt-α relative to IRMM-010 shifted when these contaminants were present. A 10/1 concentration ratio solution of Fe to Pt was also prepared due to the observation that Fe took longer to attenuate in the elution profile. Zinc is eluted right before Pt and therefore also has a higher probability to be present in the Pt fraction. For this reason 4/1 and 10/1 concentration ratio solutions of Zn to Pt were also measured.

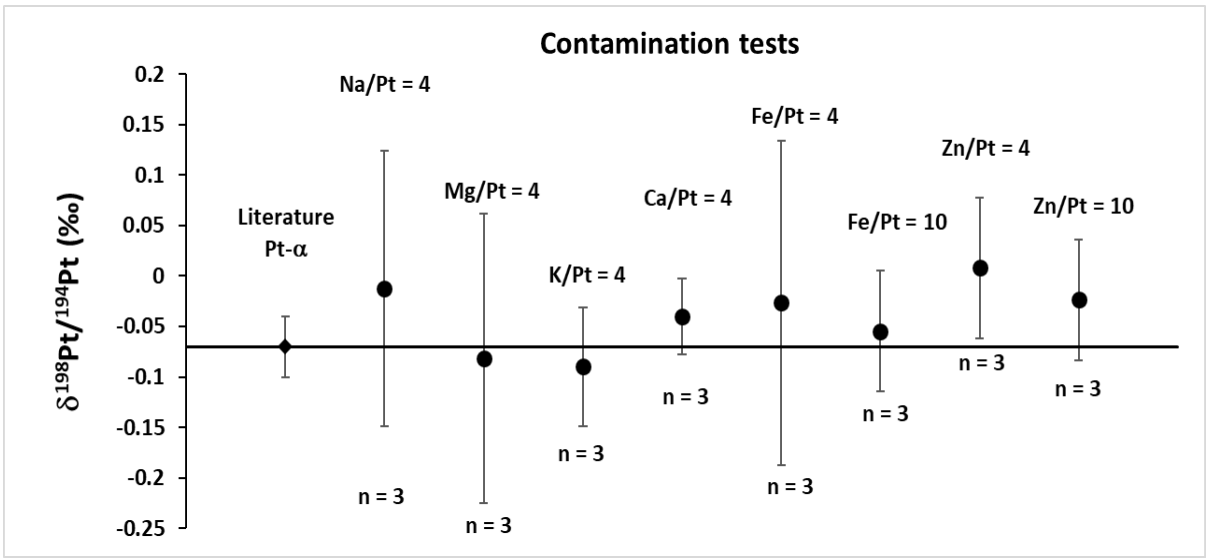

Pt-$\alpha_{IRMM-010}$ = -0.07 ± 0.03 ‰, Poole et al.[22]

Figure 14 Determined δ–values for Pt-α relative to IRMM-010 using SSB as a correction procedure when possible contaminants are present in a concentration 4-fold or 10-fold as high as the Pt concentration. The number of measurements in one session is represented by n. The error bars represent 2 * standard deviation.

Table 14 Results of the contamination tests, for which the concentration ratios of contaminant to Pt tested are represented in the first column.

Sample	Mean (‰)	2 * standard deviation	n
Literature	-0.07	0.03	
Na/Pt = 4	-0.01	0.14	3
Mg/Pt = 4	-0.08	0.14	3
K/Pt = 4	-0.09	0.06	3
Ca/Pt = 4	-0.04	0.04	3
Fe/Pt = 4	-0.03	0.16	3
Fe/Pt = 10	-0.05	0.06	3
Zn/Pt = 4	0.01	0.07	3
Zn/Pt = 10	-0.02	0.06	3

None of the contaminants seemed to heavily influence the δ-value for Pt-α relative to IRMM-010 according to the results shown in Figure and Table 14. It should be noted that due to working as precisely as possible and performing all sample preparation procedures in a class-10 clean room laboratory, contaminants were not expected to be present in the samples in these ratios.

9.4.3 Concentration mismatch test

In sample-standard bracketing, matching the concentrations of analyte in the standard and in the samples as closely as possible is necessary. The results shown in Figure and Table 15 show whether a mismatch in Pt concentration between bracketing standard and samples had an important influence on the δ-value for Pt-α.

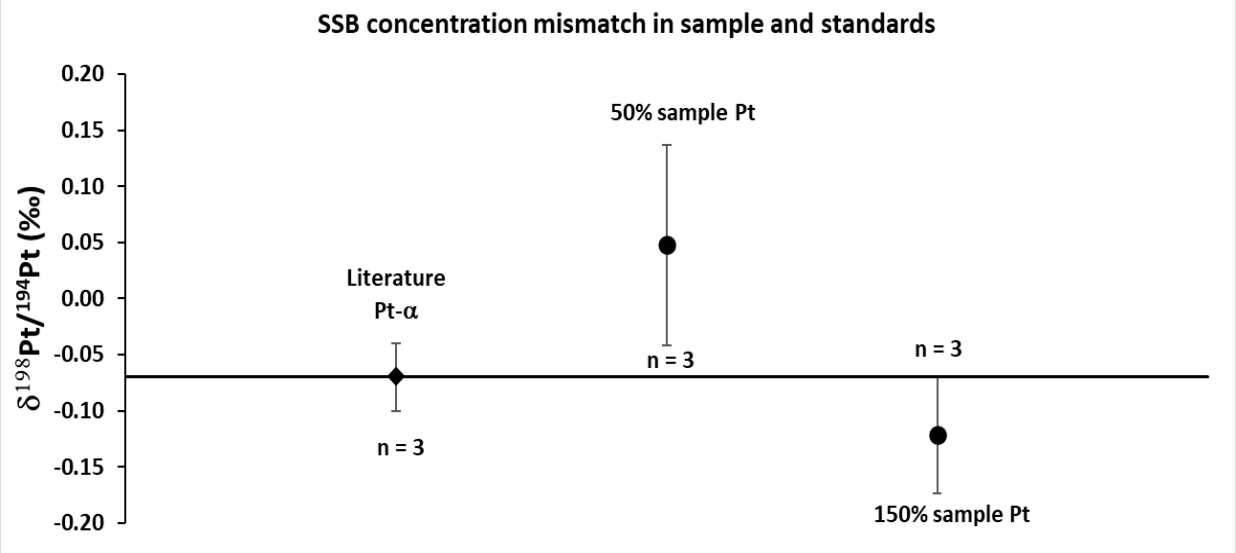

Pt-$\alpha_{IRMM-010}$ = -0.07 ± 0.03 ‰, Poole et al.[22]

Figure 15 Determined δ–values for Pt-α relative to IRMM-010 using SSB as a correction procedure when the Pt concentration in the sample is 50% or 150% of the concentration of Pt in the bracketing standard. The number of measurements in one session is represented by n. The error bars represent 2 * standard deviation.

Table 15 Results for the concentration mismatch test, where the first column represents the Pt concentration in the sample relative to the Pt concentration in the bracketing standard.

Sample	Mean (‰)	2 * standard deviation	n
Literature	-0.07	0.03	
50% Pt concentration	0.05	0.09	3
150% Pt concentration	-0.12	0.05	3

According to the results, the δ-value for Pt-α seems to be higher when the sample has a lower Pt concentration compared to the bracketing standard. Due to the lower precision however this observation was not conclusive. There might be a trend according to which the lower the Pt concentration is, the higher the δ-value will be. A higher concentration of Pt cannot be measured using this instrument, but a Pt concentration in the sample of 25% compared to the Pt concentration in the bracketing standard might be worth to measure as well. These results did show that matching the concentration when using sample-standard bracketing is important.

9.4.4 Isotopic analysis of column cut samples

After developing a chromatographic and measurement procedure, it was examined whether the chromatographic separation introduces fractionation. If the column does not cause fractionation effects, the δ-value for Pt-α that did not undergo chromatography should be the same as the δ-value for Pt-α after passing through the column. It was also examined whether Pt fractions that eluted from the column earlier had a different δ-value than Pt fractions that eluted from the column later on by collecting smaller volume cuts and analyzing these separately.

Column cut samples were treated in the following way: after the column chromatography the collected fractions were evaporated to dryness. The resin that could have come of in the fractions was destroyed by digesting the fractions in concentrated HNO_3 on a hotplate overnight, after which the samples were evaporated to dryness once again. Then, the dried samples were digested in 6 M HCl on a hotplate, to convert the samples into chloride form after which the digest was evaporated to dryness once more to finally obtain a solution in 0.5 M HCl to be measured on the Neptune.

To examine the possibility of on-column fractionation, pure Pt-α (131 ng) was loaded onto the column. 1 mL of the synthetic cell solution, containing Pt-α (98 ng), was also loaded onto the column.

To determine if there was a difference in isotopic composition of Pt leaving the column over time, 1500 ng of pure Pt-α was also loaded onto the column. For this column, the 15.6 M HNO_3 fraction was collected in 2 mL cuts instead of 4 mL cuts. This resulted in a total of ten cuts. Based on the chromatogram, it was estimated how much Pt would be in each cut so post-column dilutions could be made accordingly for measurements. Figure and Table 16 show the δ-values for both the on-column fractionation test and the smaller volume collected cuts. The Pt concentration in the final six 2 mL cuts was already too low to perform measurements.

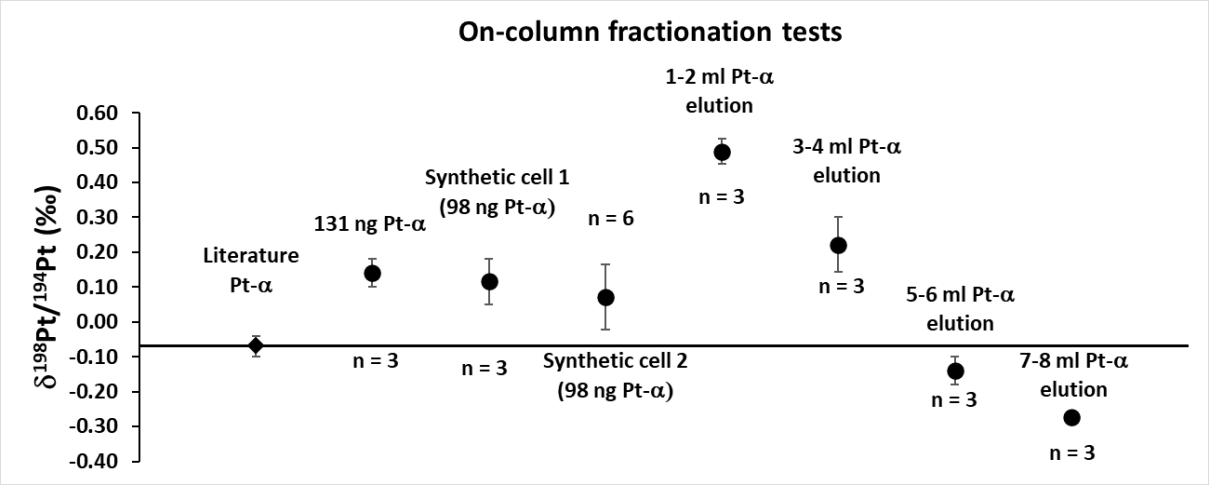

Pt-$\alpha_{IRMM-010}$ = -0.07 ± 0.03 ‰, Poole et al.[22]

Figure 16 Determined δ-values for Pt-α relative to IRMM-010 for samples that were passed through a column. The first three tests provided values for the entire Pt fraction (the 15.6 M HNO_3 fraction) of samples loaded onto the column. The final four values all stem from one chromatographic separation and represent the δ-value in the cuts collected in a smaller volume (2 mL). The number of measurements in one session is represented by n. The error bars represent 2 * standard deviation.

Table 16 Results for the column cut samples. Only the first four 2 mL cuts are represented because the Pt concentration in the following 6 cuts was not high enough to perform measurements on the Neptune.

Sample	Mean (‰)	2 * standard deviation	n
Literature	-0.07	0.03	
131 ng pure Pt-α	0.14	0.04	3
Synthetic cell 1 column	0.12	0.07	3
Synthetic cell 2 column	0.07	0.09	6
1-2 ml cut	0.49	0.04	3
3-4 ml cut	0.22	0.08	3
5-6 ml cut	-0.14	0.04	3
7-8 ml cut	-0.27	0.01	3

The δ-value for Pt-α was significantly higher whenever Pt-α was passed through a column (± 0.20 ‰ higher). The first synthetic cell sample was a sample used for the Xseries II measurement, and it compared well with the measurement for the synthetic sample of this test, showing the results are reproducible. The δ-values for the pure Pt-α solution and the synthetic cell solution were in the same range, suggesting that the other elements present in the synthetic cell solution did not influence the measurement. A possible explanation for this observation can be given by evaluating the results of the cuts collected in a smaller volume. The δ-value for the first cut was higher (0.49 ± 0.04 ‰) than the δ-value for the fourth cut (-0.27 ± 0.01 ‰). This result suggested that the heavier isotopes of Pt were eluted first. Therefore, if some Pt would be left on the column, it would be enriched in the lighter isotopes, explaining why the δ-values for Pt-α that was passed through a column were higher.

However, according to the concentration measurements on the Xseries II instrument and the elution profile, quantitative Pt recovery was achieved. Therefore, there had to be a different reason for the heavier Pt isotopic compositions after column chromatography.

Creech et al.[20] suggested that there could be (organic) contamination originating from the resin due to the high volume of concentrated HNO_3 used to elute Pt, which could possibly degrade the resin and influence the results. The post-column sample treatment used in this study is more intensive than the one used until now during this thesis. For the following measurements column-processed samples were treated in the same way as in the study by Creech et al.[20] First, the samples were evaporated to dryness and then digested in aqua regia, a mixture of 3:1 volume ratio of concentrated HCl : concentrated HNO_3, on a hotplate overnight, instead of just digesting in concentrated HNO_3. The samples were then evaporated to dryness once again and then digested in a mixture of concentrated HNO_3 and H_2O_2 (3:1 volume ratio) on a hotplate overnight. After evaporating to dryness once more, the samples were digested in 6 M HCl on a hotplate, to convert them into chloride form, after which the digest was evaporated to dryness one last time to finally obtain a solution in 0.5 M HCl to be measured on the Neptune.

9.4.5 Matrix matching by processing the standard through the column

The results of the isotopic analysis of the column cut samples led to more experimenting with samples on the column. IRMM-010 was processed on the column to use as a bracketing standard for the Pt-α samples that were passed through a column. In this way, all the effects introduced by the column chromatography would be matched in sample and bracketing standard and therefore the δ-value determined for Pt-α should be closer to the value reported in literature (-0.07 ± 0.03 ‰). The Pt fractions of all columns were collected and treated post-column by the procedure mentioned before, that was also used by Creech et al.[20] When the samples were treated with aqua regia, they turned a yellow and red color.

Several measurements were performed loading different amounts of IRMM-010 and Pt-α onto the column. First are the results of measuring IRMM-010 that was passed through a column relative to IRMM-010 that was not passed through a column. Absence of on-column fractionation would mean that the δ-value is around 0.00 ‰ since the δ-value for Pt in IRMM-010 is calculated relative to itself. Two IRMM-010 samples were loaded onto the column: a 100 ng IRMM-010 sample and a 5000 ng IRMM-010 sample. The δ-value for Pt in the 100 ng IRMM-010 sample relative to IRMM-010 that was not passed through a column was higher than 0.00 ‰ (0.11 ± 0.02 ‰). The δ-value for Pt in the 5000 ng sample however was around 0.00 ‰ (0.00 ± 0.13‰) when calculated relative to the same IRMM-010 that was not passed through a column. These results are also shown in Figure and Table 17. It is worth noting that the δ-value for the 100 ng IRMM-010 sample was comparable to the δ-value for Pt-α and the synthetic standard from the on-column fractionation tests (0.14 ± 0.04 ‰ and 0.07 ± 0.09 ‰ respectively).

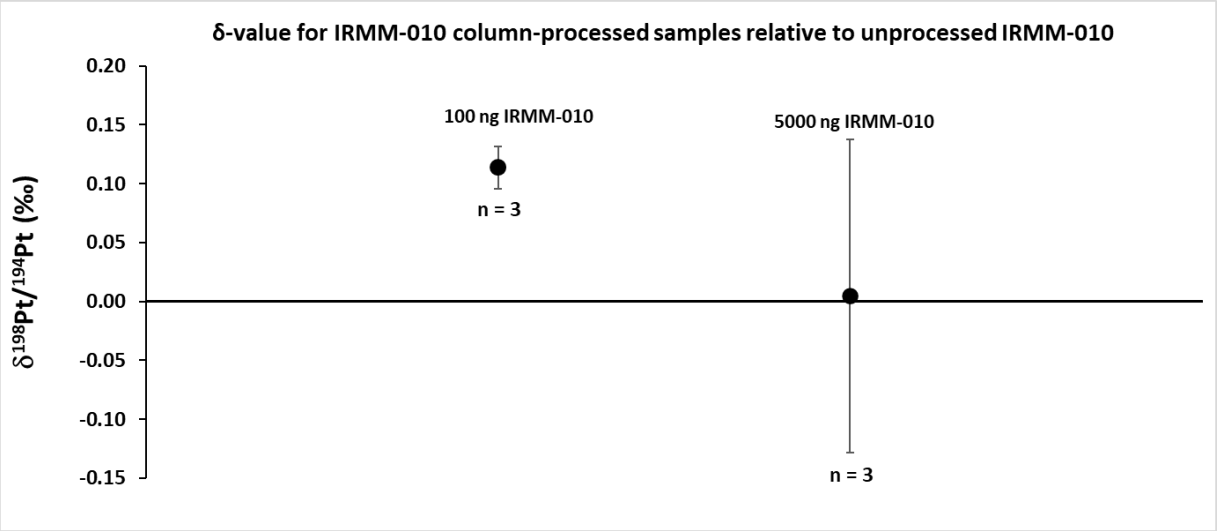

Figure 17 Determined δ–values of IRMM-010 samples that were passed through a column relative to IRMM-010 that was not passed through a column using SSB as a correction procedure. The number of measurements in one session is represented by n. The error bars represent 2 * standard deviation.

Table 17 Pt δ-values of IRMM-010 samples that were passed through a column relative to IRMM-010 that was not passed through a column.

Bracketing standard: unprocessed IRMM-010			
Sample	Mean (‰)	2 * standard deviation	n
100 ng IRMM-010	0.11	0.02	3
5000 ng IRMM-010	0.00	0.13	3

After, the Pt-α samples that were passed through a column were measured against the IRMM-010 counterpart samples that were passed through a column as bracketing standard. The matrix of the samples was now essentially matched, so the δ-value for Pt in the Pt-α should be closer to -0.07 ‰. The 100 ng Pt-α sample showed a higher δ-value for Pt than expected (0.18 ± 0.03 ‰). The δ-value for Pt in the 5000 ng Pt-α sample measured relative to 5000 ng IRMM-010 that was passed through a column was closer (-0.02 ± 0.11 ‰) to the literature value however. The 100 ng Pt-α sample was also measured against the 5000 ng IRMM-010 sample as bracketing standard to examine if this would provide a proper result for the 100 ng Pt-α sample, but this resulted in an even higher δ-value (0.27 ± 0.06 ‰) for the 100 ng Pt-α sample.

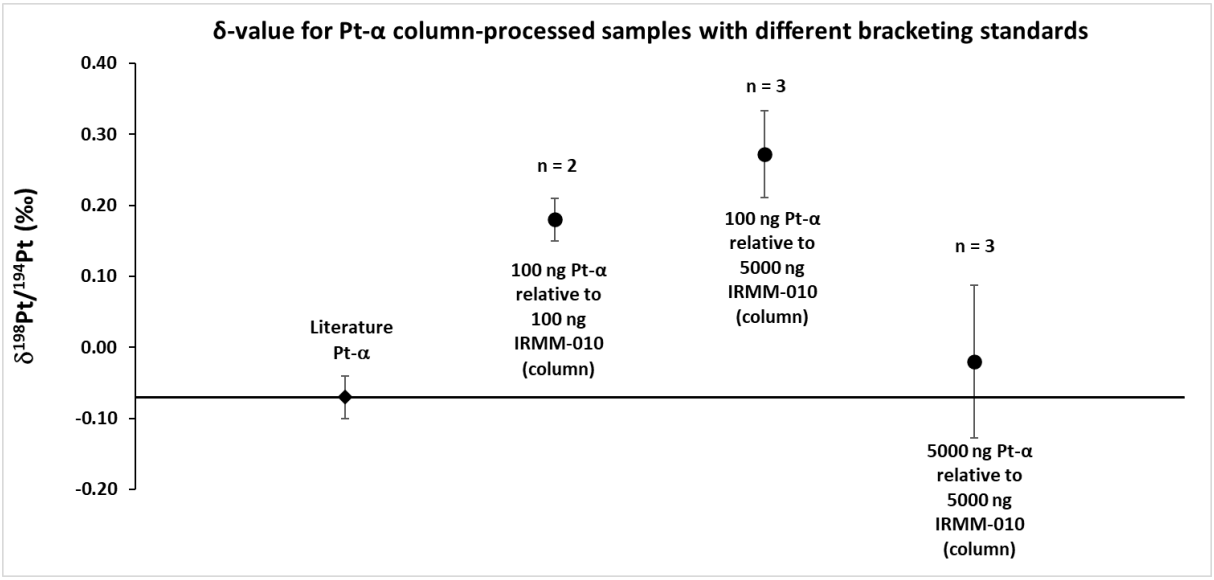

Pt-$\alpha_{IRMM-010}$ = -0.07 ± 0.03 ‰, Poole et al.[22]

Figure 18 Determined δ–values for Pt-α samples that were passed through a column relative to IRMM-010 that was also passed through a column using SSB as a correction procedure. The number of measurements in one session is represented by n. The error bars represent 2 * standard deviation.

Table 18 δ-values for Pt-α samples that were passed through a column relative to IRMM-010 that was also passed through a column.

Bracketing standard: 100 ng IRMM-010 (column)			
Sample	Mean (‰)	2 * standard deviation	n
Literature	-0.07	0.03	
100 ng Pt-α	0.18	0.03	2
Bracketing standard: 5000 ng IRMM-010 (column)			
Sample	Mean (‰)	2 * standard deviation	n
Literature	-0.07	0.03	
100 ng Pt-α	0.27	0.06	3
5000 ng Pt-α	-0.02	0.11	3

The combined results obtained until now suggest that higher δ-values are obtained when smaller amounts of Pt are loaded onto the column. To confirm this observation, the 5000 ng Pt-α sample was measured against IRMM-010 that was not passed through a column as bracketing standard. The δ-value measured for the 5000 ng Pt-α sample was -0.10 ± 0.09 ‰, which is similar to the result for Pt-α that was not processed on the column and the literature value. This result also suggested that there was no on-column fractionation when a higher amount of Pt-α was loaded onto the column. For comparison, Figure and Table 19 also include the result of a previous test (isotopic analysis of column cut samples), in which only 131 ng Pt-α was loaded onto the column and the δ-value was also calculated relative to IRMM-010 that was not passed through a column.

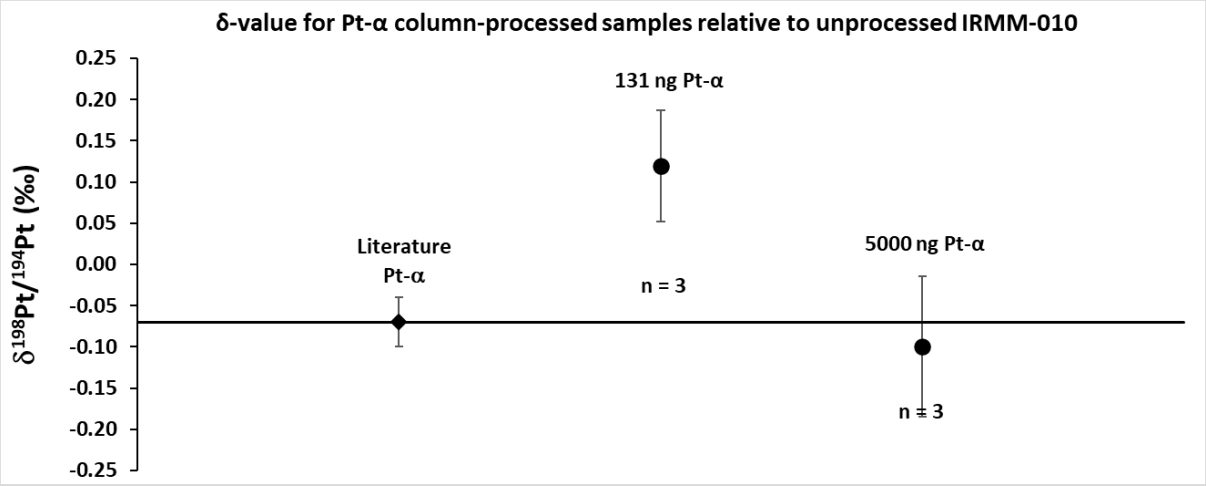

Pt-α$_{IRMM-010}$ = -0.07 ± 0.03 ‰, Poole et al.[22]

Figure 19 Determined δ–values for Pt-α samples that were passed through a column relative to IRMM-010 that was not passed through a column using SSB as a correction procedure. The number of measurements in one session is represented by n. The error bars represent 2 * standard deviation.

Table 19 Comparison of δ-values for Pt-α relative to IRMM-010 that was not passed through a column when a small amount of Pt-α was loaded (result of on-column fractionation test) versus when a large amount of Pt-α was loaded.

Bracketing standard: unprocessed IRMM-010			
Sample	Mean (‰)	2 * standard deviation	n
Literature	-0.07	0.03	
131 ng Pt-α	0.12	0.07	3
5000 ng Pt-α	-0.10	0.09	3

The synthetic standard, prepared using Pt-α, and a seronorm + Pt-α sample were also measured against the 5000 ng IRMM-010 that was passed through a column as bracketing standard. The δ-values were also higher compared to the value from literature. Just like the previous samples where this observation was made, a small amount of Pt was loaded onto the column.

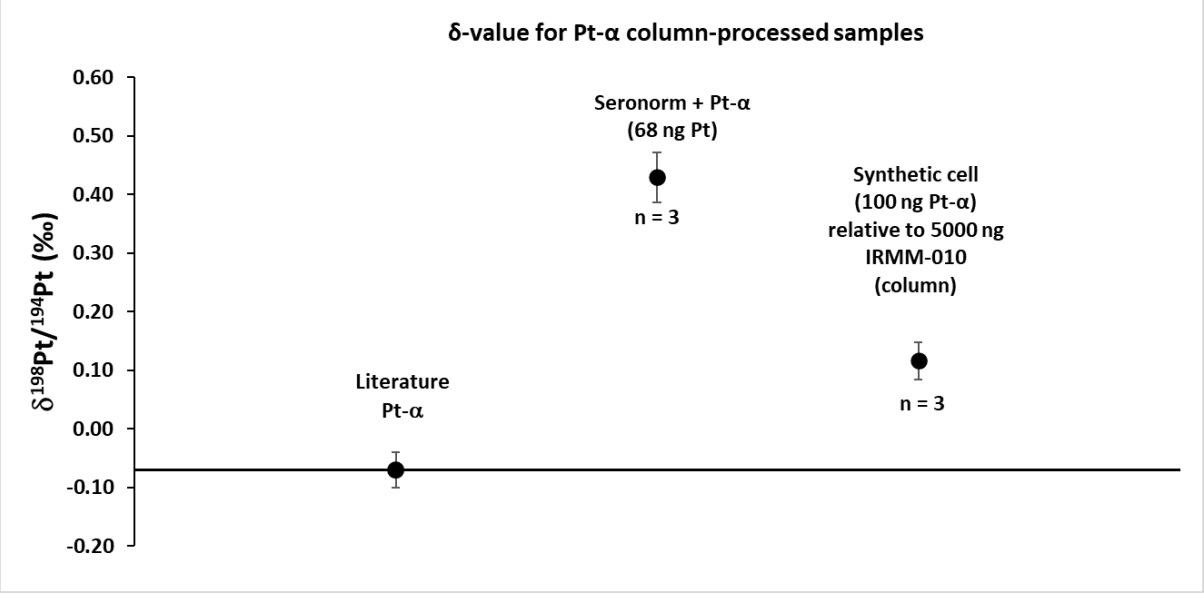

Pt-$\alpha_{IRMM-010}$ = -0.07 ± 0.03 ‰, Poole et al.[22]

Figure 20 Determined δ–values of the Seronorm + Pt-α and synthetic cell samples that were passed through a column relative to IRMM-010 that was passed through a column using SSB as a correction procedure. The number of measurements in one session is represented by n. The error bars represent 2 * standard deviation.

Table 20 δ-values of the synthetic cell and Seronorm + Pt-α samples that were passed through a column relative to IRMM-010 that was passed through a column.

Bracketing standard: 5000 ng IRMM-010 (column)			
Sample	Mean (‰)	2 * standard deviation	n
Literature	-0.07	0.03	
Seronorm + Pt-α	0.43	0.04	3
Synthetic cell	0.12	0.03	3

Based on these matrix matching results, column chromatography did not cause fractionation effects whenever a large amount of Pt was loaded onto the column. These results therefore pointed towards a contamination that is introduced by the column. The contamination/Pt ratio could be a lot higher in the samples where only ± 100 ng Pt was loaded onto the column and therefore the contamination would affect these samples a lot more, leading to a δ-value that is higher compared to the value from literature.

9.4.6 Mass-independent fractionation?

One interesting property that was also examined during this thesis was the potential occurrence of mass-independent isotope fractionation of Pt. Usually the variation in isotope ratios is directly proportional to the difference in mass of the isotopes that are involved.[49] This was tested for the $^{198}Pt/^{194}Pt$ and $^{196}Pt/^{194}Pt$ ratio. The mass difference between ^{198}Pt and ^{194}Pt is twice as large as the mass difference between ^{196}Pt and ^{194}Pt. If only mass-dependent fractionation occurs, the $\delta^{198}Pt$ value will be twice as large as the $\delta^{196}Pt$ value.

The $\delta^{198}Pt$ and $\delta^{196}Pt$ values obtained for Pt-α samples measured during this thesis are represented in Figure 21 in a three-isotope plot.

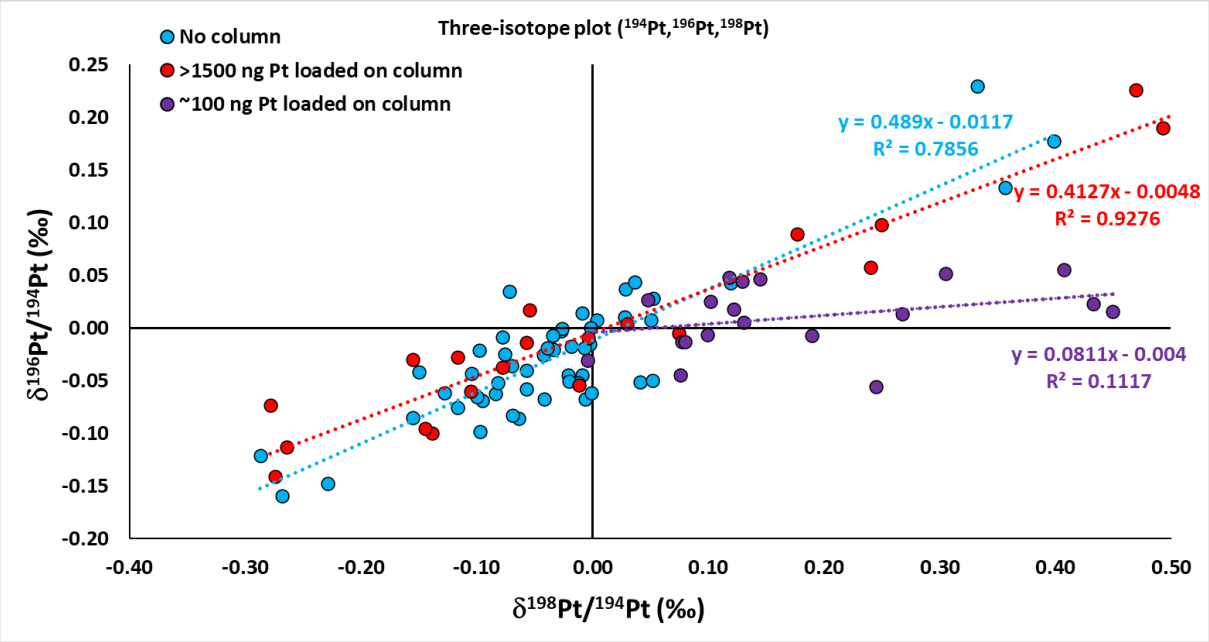

Figure 21 Three-isotope plot showing the correlation between $\delta^{198}Pt$ and $\delta^{196}Pt$.

A clear difference is observed between samples for which a low amount of Pt is loaded onto the column compared to the samples for which a high amount of Pt is loaded onto the column. The samples for which a high amount of Pt is loaded onto the column seemed to show mass-dependent isotope fractionation, whilst the samples for which a low amount of Pt was loaded did not show a clear trend, reinforcing the suspicion that some form of contamination was introduced by the column and that this contamination had an influence on the determination of several Pt δ-values. Further reinforcing this suspicion of possible contamination is that any ratio involving ^{198}Pt displayed the same behavior, suggesting that the contamination would be present at a m/z ratio of 198.

9.5 Characterization of the Pt fractions + cell samples using the Agilent Technologies 8800 ICP-MS/MS instrument

Due to the observation of a possible unknown contamination, the Pt fractions of the column-processed samples from section 9.4.5 (except the seronorm + Pt-α sample), that were eluted from the column were tested for more impurities that we did not account for at first. These were impurities / elements that were not present in the composition of the synthetic cell solution, but that could have been introduced during the column chromatography. For this test, a different stock solution was used to prepare calibration standards. This stock solution contained more elements than the stock solution used before, which only contained the elements present in the synthetic cell. The measured extra elements and the concentration of these elements in the calibration standards are presented in Table 21.

Table 21 The additional elements present in the new calibration standards and their concentration. The elements present in the synthetic cell solution and Ga are also present in these calibration standards at the concentrations shown in Table 4.

Cal. Std #	Li (µg/L)	Al (µg/L)	Ti (µg/L)	Cr (µg/L)	Mn (µg/L)	Co (µg/L)	Ni (µg/L)	Ag (µg/L)	Cd (µg/L)	Tl (µg/L)	Pb (µg/L)
0	0.0	0.0	0.0	0.0	0.0	0.0	0.0	0.0	0.0	0.0	0.0
1	0.1	0.5	0.5	0.2	0.1	0.2	0.5	0.2	0.2	0.2	0.2
2	0.5	2.5	2.5	1.0	0.5	1.0	2.5	1.0	1.0	1.0	1.0
3	1.0	4.9	4.9	2.0	1.0	2.0	4.9	2.0	2.0	2.0	2.0
4	2.5	12.3	12.3	4.9	2.5	4.9	12.3	4.9	5.1	4.9	4.9
5	4.9	24.7	24.7	9.9	4.9	9.9	24.6	9.9	10.1	9.9	9.9

Furthermore, even if the focus was no longer on measuring Pt isotope ratios in the A2780(cis) cell samples, it would already be useful to characterize two A2780 and two A2780cis cell samples that were all treated with cisplatin. Based on a previous measurement where the concentration of all the elements was too high, dilutions to measure the concentration of several elements, including Pt, were made accordingly. The four cell samples were characterized using the 8800 ICP-MS/MS instrument.

Instrument settings for the 8800 ICP-MS/MS instrument can be found in Table 22.

Table 22 Agilent 8800 ICP-MS/MS operating conditions.

Instrument settings	
Sample uptake rate	0.35 mL min^{-1}
Plasma gas flow rate	15.0 L Ar min^{-1}
Auxiliary gas flow rate	0.9 L Ar min^{-1}
Nebulizer gas flow rate	~ 1.12 L Ar min^{-1}
Collision gas flow rate	1.0 mL He min^{-1}
Reaction gas flow rate	1.00 mL CH_3F/He (10%/90%) min^{-1}
RF power	1550 W
Sample cone	Ni tip with Cu base
Skimmer cone	Ni
Data acquisition parameters	
Integration time	1 s
Replicates	10
Sweeps	100

The column-processed samples from section 9.4.5 (except the seronorm + Pt-α sample) were diluted to a Pt concentration of 5 µg/L. Using the dilution factor, the amount of Pt in the samples (in ng) was calculated. These amounts and the Pt yield after column chromatography are shown in Table 23.

Table 23 Amount of Pt recovered after column chromatography (in ng) and yield (in %).

Sample	Amount of Pt in sample (ng)	Pt yield after column chromatography (%)
100ng IRMM Pt	91	91
100ng Pt-α	95	95
5000ng IRMM Pt	4870	97
5000ng Pt-α	4940	99
SynthCell Pt-α	94	96

Other elements, present in the new calibration standards, were also measured in these Pt fractions to see if a possible contaminant could already be determined. These element/Pt concentration ratios are presented in Tables 24, 25 and 26. The K concentration was not determined using the Agilent 8800 instrument due to lack of NH_3 as reaction gas. To determine the concentration of K in the 5000 ng IRMM Pt sample, the signal intensity of a 100 µg/L K standard was measured on the Neptune and compared to the signal intensity in this sample. If the concentration of the element was below the detection limit, the ratio will be represented in the table by "< DL" or lower than detection limit.

Table 24 Element/Pt concentration ratios of Li, Na, Mg, Al, Ca and Ti in the column-processed samples.

Sample	Li	Na	Mg	Al	Ca	Ti
100ng IRMM Pt	0.03	0.17	0.14	0.20	0.41	< DL
100ng Pt-α	0.05	0.09	0.17	0.18	0.34	< DL
5000ng IRMM Pt	< DL	0.03	0.02	0.03	0.29	< DL
5000ng Pt-α	< DL	0.69	0.01	0.04	0.32	< DL
SynthCell Pt-α	< DL	0.20	0.14	0.35	0.70	< DL

Table 25 Element/Pt concentration ratios of Cr, Mn, Fe, Co, Ni and Cu in the column-processed samples.

Sample	Cr	Mn	Fe	Co	Ni	Cu
100ng IRMM Pt	0.05	0.00	0.12	0.01	0.02	0.01
100ng Pt-α	0.05	0.00	0.09	0.01	0.02	0.00
5000ng IRMM Pt	0.01	0.00	0.02	0.00	0.02	0.00
5000ng Pt-α	0.01	0.00	0.04	0.00	0.02	0.00
SynthCell Pt-α	0.05	0.00	0.12	0.01	0.01	0.01

Table 26 Element/Pt concentration ratios of Zn, Ag, Cd, Tl, Pb and K in the column-processed samples.

Sample	Zn	Ag	Cd	Tl	Pb	K
100ng IRMM Pt	0.02	0.16	0.00	0.00	0.02	
100ng Pt-α	0.03	0.15	0.00	0.00	0.01	
5000ng IRMM Pt	0.01	0.15	0.00	0.00	0.01	0.12
5000ng Pt-α	0.01	0.16	0.00	0.00	0.02	
SynthCell Pt-α	0.06	0.16	0.00	0.00	0.03	

The element/Pt concentration ratios were low and similar in all the samples. From the results of the previous contamination tests, it was already concluded that for some of these elements a 4/1 concentration ratio did not influence the δ-value for Pt-α and these ratios are lower, so individually they would not have caused the shift to higher δ-values.

The four analyzed A2780(cis) cell samples were all treated with cisplatin. Samples 1 and 2 are A2780cis cell samples treated with cisplatin, whilst samples 3 and 4 are regular A2780 cell samples treated with cisplatin. Tables 27 and 28 show the amount of biologically relevant elements (elements in the synthetic cell solution) present in the samples. Potassium could not be measured due to the lack of NH_3 as reaction gas. The precision is expressed in terms of %RSD. Information on the number of cells, or the mass of the cell samples before digestion was not available, so these amounts could not be normalized and reported as concentration values.

Table 27 Amount of Na in µg and Mg, Ca and Fe in ng in 4 of the cell samples.

	Na		Mg		Ca		Fe	
Sample	Mass (µg)	%RSD	Mass (ng)	%RSD	Mass (ng)	%RSD	Mass (ng)	%RSD
1	2,554	7.0	4,351	7.4	1,236	4.2	279	11
2	3,097	9.1	10,760	6.1	3,038	7.4	207	16
3	270	7.9	19,472	8.4	8,780	3.8	350	13
4	3,212	7.8	18,931	9.1	11,181	2.3	581	16

Table 28 Amount of Cu, Zn and Pt in ng in 4 of the cell samples.

	Cu		Zn		Pt	
Sample	Mass (ng)	%RSD	Mass (ng)	%RSD	Mass (ng)	%RSD
1	14	2.0	221	7.8	56	1.3
2	18	2.4	591	9.5	57	2.0
3	52	2.9	1,210	6.8	211	1.8
4	54	1.9	1,374	6.8	249	1.6

The divergent value for Na in sample 3 is most likely due to a different way of collecting the cell sample compared to that for samples 1, 2 and 4. One interesting observation that can be made based on these results is that samples 3 and 4 have higher amounts of metals in the cells compared to samples 1 and 2. Samples 1 and 2 are the cisplatin resistant cells, and apparently, not only the Pt uptake is lowered when cells are resistant to cisplatin. In the introduction of this thesis, it was already mentioned that there is a significant correlation between high-affinity Cu uptake protein 1 (CTR1) expression and cisplatin accumulation in the A2780 and A2780cis ovarian cancer cell lines, demonstrating a link between Cu homeostasis and cisplatin uptake.[18] This, together with the observations made from Tables 27 and 28, could suggest that Pt is transported into the cells using uptake proteins that also transport other metals into the cells. These uptake proteins could be less expressed in the A2780cis cells, which causes less Pt uptake and less uptake for the other elements as well.

The Agilent Technologies 8800 ICP-MS/MS instrument was used for the concentration measurements because interferences are removed very efficiently by this instrument. This is because this instrument is a tandem ICP-MS set-up, as explained in the research plan section. Aluminum is an excellent example to better explain how this works. Methylfluoride (CH_3F) was used as a reaction gas. The first quadrupole filters out every ion which does not have an m/z ratio of 27. In the collision/reaction cell, also containing a quadrupole, the $^{27}Al^+$ ions are converted into $AlCH_3F^+$ reaction product ions with an m/z ratio of 61. The third and final quadrupole will only allow ions with an m/z ratio of 61 to pass. In

this way only the Al reaction product ions reach the detector, since other ions with an m/z ratio of 61 were already removed by the first quadrupole. This approach is also known as the mass shift approach and is explained more in detail in Bolea-Fernandez et al.[50]

9.5.1 Method validation for element quantification

The trace metal concentrations in the reference material Seronorm Serum L-1 were also determined using the Agilent 8800 ICP-MS/MS instrument. These concentrations were compared to the reference values to prove the validity of the measurement procedure used in this thesis. The results are shown in Tables 29 and 30. The precision on the sample measurements is expressed in terms of %RSD. The results of the reference values are represented together with the 95 % confidence interval.

Table 29 Measured concentrations for Na, Mg and Ca (in mg/L) in Seronorm Serum L-1 compared to the reference values (with 95 % confidence interval) of these elements

	Na		Mg		Ca	
	concentration (mg/L)	%RSD	concentration (mg/L)	%RSD	concentration (mg/L)	%RSD
Sample	2,590	1.5	21.5	2.8	55	3.1
Reference value	3,855 ± 776		19.3 ± 3.9		97 ± 20	

Table 30 Measured concentrations for Fe (in mg/L), Cu (in µg/L) and Zn (in mg/L) in Seronorm Serum L-1 compared to the reference values (with 95 % confidence interval) of these elements

	Fe		Cu		Zn	
	concentration (mg/L)	%RSD	concentration (µg/L)	%RSD	concentration (mg/L)	%RSD
Sample	1.41	3.5	1,070	0.55	1.41	3.7
Reference value	1.40 ± 0.28		1,128 ± 227		1.46 ± 0.29	

The measured values were in the range of the 95% confidence interval for Mg, Fe, Cu and Zn. An intermediate solution was prepared to determine the Na concentration, which could be a possible explanation for the low concentration value that was measured (the intermediate solution was possibly not mixed homogenously). Ca was measured in the same sample as Mg, so this divergent value cannot immediately be explained.

9.6 IC-50 tests in A2780 and A2780cis cells

Most of the cell work, or the third work package, included preparing the cell samples. This involved determination of the IC-50, or the half maximal inhibitory concentration of cisplatin for both the A2780 cells and A2780cis cells. This is the concentration of cisplatin that leads to half of the cells being inhibited or inactive. The cells were seeded at a density of 4×10^3 cells/well in 96-well plates, grown for 24 hours and then exposed to cisplatin for 72 hours at various concentration levels ranging from 0 to 25 µM of cisplatin. This method was also used by Schoeberl et al.[18] The cell viability was then determined using a CellTiter-Glo assay. The results of this test and the results published by Schoeberl et al.[18] are represented in Table 31.

Table 31 Comparison of IC-50 values for A2780 and A2780cis cells determined in this work to the values determined by Schoeberl et al.[18]

	A2780			A2780cis		
Measurement	IC-50 (µM)	Stdev	n	IC-50 (µM)	Stdev	n
this work	0.95	0.25	3	9.51	1.99	3
Schoeberl et al.[18]	1.56	0.31		6.87	1.13	

10. Outlook

Ultimately, the final stage of Pt isotopic analysis of the cell samples (work package 4) was not reached. As mentioned before, the cell samples are precious and reliable results can only be obtained when all the factors that could influence the results are determined and can be avoided or adequately corrected for. One of the first observations during this thesis that was not mentioned in literature was the change of color of the AG1-X8 resin from yellow to red when using concentrated HNO_3 in the chromatographic procedure. This could already be a reason for results that are different from those reported in the literature. A different resin could possibly provide a solution for this problem. The AG MP-1M anion exchange resin behaves similarly as the AG1-X8 anion exchange resin and a quick test using the AG MP-1M resin showed that this resin did not change color when using concentrated HNO_3. This gives a viable reason to check whether this resin can be used for Pt chromatography instead of the AG1-X8 resin and if this would provide better results. The chromatographic procedure also shows that Zn is separated from the matrix elements and this procedure could therefore also be used as a basis for Zn isotopic analysis. The measurements using the Agilent 8800 ICP-MS/MS unit also showed that some unexpected elements like Al, Ag or Pb could be present in the samples after chromatography and these elements could possibly influence the δ-value. Although these observations could have been an instrument background issue, it should be checked if the current chromatographic procedure can separate larger amounts of these elements from Pt as well. Perhaps the SSB correction is insufficient when working with these small amounts of Pt and Pt double spike correction could help correct biased Pt isotope ratios adequately, potentially enabling a higher precision as well. Eventually all these improvements could make it possible to determine the Pt isotopic composition of the cell samples. Although this thesis was not able to determine whether resistance to cisplatin affects Pt isotope fractionation, it does provide a solid basis for future research in Pt isotopic analysis in the context of ovarian cancer.

References

(1) Dawson, T. E.; Brooks, P. D. Fundamentals of stable isotope chemistry and measurement. *Stable isotope techniques in the study of biological processes and functioning of ecosystems* **2001**, 1-18.
(2) Wiederhold, J. G. Metal stable isotope signatures as tracers in environmental geochemistry. *Environmental science & technology* **2015**, *49* (5), 2606-2624.
(3) Albarède, F. Metal stable isotopes in the human body: a tribute of geochemistry to medicine. *Elements* **2015**, *11* (4), 265-269.
(4) Mahan, B.; Chung, R. S.; Pountney, D. L.; Moynier, F.; Turner, S. Isotope metallomics approaches for medical research. *Cellular and Molecular Life Sciences* **2020**, *77* (17), 3293-3309. DOI: 10.1007/s00018-020-03484-0.
(5) Vanhaecke, F.; Costas-Rodríguez, M. High-precision isotopic analysis of essential mineral elements: capabilities as a diagnostic/prognostic tool. *View* **2021**, *2* (1), 20200094.
(6) Sullivan, K. V.; Moore, R. E. T.; Vanhaecke, F. The influence of physiological and lifestyle factors on essential mineral element isotopic compositions in the human body: implications for the design of isotope metallomics research. *Metallomics* **2023**, *15* (3). DOI: 10.1093/mtomcs/mfad012 (acccessed 4/30/2023).
(7) Morgan, R. J.; Armstrong, D. K.; Alvarez, R. D.; Bakkum-Gamez, J. N.; Behbakht, K.; Chen, L.-m.; Copeland, L.; Crispens, M. A.; DeRosa, M.; Dorigo, O. Ovarian cancer, version 1.2016, NCCN clinical practice guidelines in oncology. *Journal of the National Comprehensive Cancer Network* **2016**, *14* (9), 1134-1163.
(8) Henderson, J. T.; Webber, E. M.; Sawaya, G. F. Screening for ovarian cancer: updated evidence report and systematic review for the US preventive services task force. *Jama* **2018**, *319* (6), 595-606.
(9) Rosen, D. G.; Wang, L.; Atkinson, J. N.; Yu, Y.; Lu, K. H.; Diamandis, E. P.; Hellstrom, I.; Mok, S. C.; Liu, J.; Bast Jr, R. C. Potential markers that complement expression of CA125 in epithelial ovarian cancer. *Gynecologic oncology* **2005**, *99* (2), 267-277.
(10) Sopik, V.; Rosen, B.; Giannakeas, V.; Narod, S. A. Why have ovarian cancer mortality rates declined? Part III. Prospects for the future. *Gynecologic Oncology* **2015**, *138* (3), 757-761.
(11) Pinsky, P. F.; Yu, K.; Kramer, B. S.; Black, A.; Buys, S. S.; Partridge, E.; Gohagan, J.; Berg, C. D.; Prorok, P. C. Extended mortality results for ovarian cancer screening in the PLCO trial with median 15 years follow-up. *Gynecologic oncology* **2016**, *143* (2), 270-275.
(12) Meyer, T.; Rustin, G. J. Role of tumour markers in monitoring epithelial ovarian cancer. *British journal of cancer* **2000**, *82* (9), 1535-1538.
(13) Lippert, T. H.; Ruoff, H.-J.; Volm, M. Current status of methods to assess cancer drug resistance. *International journal of medical sciences* **2011**, *8* (3), 245.
(14) van Zyl, B.; Tang, D.; Bowden, N. A. Biomarkers of platinum resistance in ovarian cancer: what can we use to improve treatment. *Endocrine-related cancer* **2018**, *25* (5), R303-R318.
(15) Kilari, D.; Guancial, E.; Kim, E. S. Role of copper transporters in platinum resistance. *World journal of clinical oncology* **2016**, *7* (1), 106.
(16) Krizkova, S.; Ryvolova, M.; Hrabeta, J.; Adam, V.; Stiborova, M.; Eckschlager, T.; Kizek, R. Metallothioneins and zinc in cancer diagnosis and therapy. *Drug Metabolism Reviews* **2012**, *44* (4), 287-301.
(17) Kischel, P.; Girault, A.; Rodat-Despoix, L.; Chamlali, M.; Radoslavova, S.; Abou Daya, H.; Lefebvre, T.; Foulon, A.; Rybarczyk, P.; Hague, F. Ion channels: New actors playing in chemotherapeutic resistance. *Cancers* **2019**, *11* (3), 376.
(18) Schoeberl, A.; Gutmann, M.; Theiner, S.; Corte-Rodríguez, M.; Braun, G.; Vician, P.; Berger, W.; Koellensperger, G. The copper transporter CTR1 and cisplatin accumulation at the single-cell level by LA-ICP-TOFMS. *Frontiers in Molecular Biosciences* **2022**, 1303.
(19) Cadiou, J.-L. Copper transporters are responsible for copper isotopic fractionation in eukaryotic cells. PhD thesis, Université de Lyon, 2017.

(20) Creech, J. B.; Baker, J. A.; Handler, M. R.; Bizzarroc, M. Platinum stable isotope analysis of geological standard reference materials by double-spike MC-ICPMS. *Chemical Geology* **2014**, *363*, 293-300. DOI: 10.1016/j.chemgeo.2013.11.009.
(21) Creech, J.; Baker, J.; Handler, M.; Lorand, J.-P.; Storey, M.; Wainwright, A.; Luguet, A.; Moynier, F.; Bizzarro, M. Late accretion history of the terrestrial planets inferred from platinum stable isotopes. *Geochem. Perspect. Lett* **2017**, *3*, n1.
(22) Poole, G. M.; Stumpf, R.; Rehkämper, M. New methods for determination of the mass-independent and mass-dependent platinum isotope compositions of iron meteorites by MC-ICP-MS. *Journal of Analytical Atomic Spectrometry* **2022**, *37* (4), 783-794.
(23) Linge, K. L.; Jarvis, K. E. Quadrupole ICP-MS: Introduction to instrumentation, measurement techniques and analytical capabilities. *Geostandards and geoanalytical research* **2009**, *33* (4), 445-467.
(24) Greber, N.; Van Zuilen, K. Multi-collector inductively coupled plasma mass spectrometry: new developments and basic concepts for high-precision measurements of mass-dependent isotope signatures. *Chimia* **2022**, *76* (1-2), 18-18.
(25) Brand, W. A.; Coplen, T. B. Stable isotope deltas: tiny, yet robust signatures in nature. *Isotopes in environmental and health studies* **2012**, *48* (3), 393-409.
(26) Balcaen, L.; Bolea-Fernandez, E.; Resano, M.; Vanhaecke, F. Inductively coupled plasma–Tandem mass spectrometry (ICP-MS/MS): A powerful and universal tool for the interference-free determination of (ultra) trace elements–A tutorial review. *Analytica chimica acta* **2015**, *894*, 7-19.
(27) Pearson, D.; Woodland, S. Solvent extraction/anion exchange separation and determination of PGEs (Os, Ir, Pt, Pd, Ru) and Re–Os isotopes in geological samples by isotope dilution ICP-MS. *Chemical Geology* **2000**, *165* (1-2), 87-107.
(28) Poole, C. F. *The essence of chromatography*; Elsevier, 2003.
(29) Morgan, J. L.; Skulan, J. L.; Gordon, G. W.; Romaniello, S. J.; Smith, S. M.; Anbar, A. D. Rapidly assessing changes in bone mineral balance using natural stable calcium isotopes. *Proceedings of the National Academy of Sciences* **2012**, *109* (25), 9989-9994.
(30) Toubhans, B.; Gourlan, A.; Telouk, P.; Lutchman-Singh, K.; Francis, L.; Conlan, R.; Margarit, L.; Gonzalez, D.; Charlet, L. Cu isotope ratios are meaningful in ovarian cancer diagnosis. *Journal of Trace Elements in Medicine and Biology* **2020**, *62*, 126611.
(31) Rabinowitz, J. D.; Enerbäck, S. Lactate: the ugly duckling of energy metabolism. *Nature Metabolism* **2020**, *2* (7), 566-571.
(32) Fox, L. Carboplatin. *J Am Anim Hosp Assoc* **2000**, *36* (1), 13-14.
(33) Ghosh, S. Cisplatin: The first metal based anticancer drug. *Bioorganic chemistry* **2019**, *88*, 102925.
(34) Pavelka, M.; Lucas, M. F. A.; Russo, N. On the hydrolysis mechanism of the second-generation anticancer drug carboplatin. *Chemistry–A European Journal* **2007**, *13* (36), 10108-10116.
(35) Zhang, C.; Xu, C.; Gao, X.; Yao, Q. Platinum-based drugs for cancer therapy and anti-tumor strategies. *Theranostics* **2022**, *12* (5), 2115.
(36) Michalke, B. Platinum speciation used for elucidating activation or inhibition of Pt-containing anti-cancer drugs. *Journal of Trace Elements in Medicine and Biology* **2010**, *24* (2), 69-77.
(37) Di Pasqua, A. J.; Goodisman, J.; Dabrowiak, J. C. Understanding how the platinum anticancer drug carboplatin works: From the bottle to the cell. *Inorganica Chimica Acta* **2012**, *389*, 29-35.
(38) Crider, S. E.; Holbrook, R. J.; Franz, K. J. Coordination of platinum therapeutic agents to met-rich motifs of human copper transport protein1. *Metallomics* **2010**, *2* (1), 74-83.
(39) Viscarra, T.; Buchegger, K.; Jofre, I.; Riquelme, I.; Zanella, L.; Abanto, M.; Parker, A. C.; Piccolo, S. R.; Roa, J. C.; Ili, C. Functional and transcriptomic characterization of carboplatin-resistant A2780 ovarian cancer cell line. *Biological Research* **2019**, *52* (1), 1-13.
(40) Maréchal, C. N.; Télouk, P.; Albarède, F. Precise analysis of copper and zinc isotopic compositions by plasma-source mass spectrometry. *Chemical geology* **1999**, *156* (1-4), 251-273.
(41) Kidder, J. A.; Voinot, A.; Sullivan, K. V.; Chipley, D.; Valentino, M.; Layton-Matthews, D.; Leybourne, M. Improved ion-exchange column chromatography for Cu purification from high-Na matrices and isotopic analysis by MC-ICPMS. *Journal of Analytical Atomic Spectrometry* **2020**, *35* (4), 776-783.

(42) Breton, T.; Lloyd, N. S.; Trinquier, A.; Bouman, C.; Schwieters, J. B. Improving precision and signal/noise ratios for MC-ICP-MS. *Procedia Earth and Planetary Science* **2015**, *13*, 240-243.
(43) Creech, J. B.; Schaefer, B. F.; Turner, S. P. Application of 1013 Ω Amplifiers in Low-Signal Plasma-Source Isotope Ratio Measurements by MC-ICP-MS: A Case Study with Pt Isotopes. *Geostandards and Geoanalytical Research* **2020**, *44* (2), 223-229.
(44) Baxter, D. C.; Rodushkin, I.; Engström, E.; Malinovsky, D. Revised exponential model for mass bias correction using an internal standard for isotope abundance ratio measurements by multi-collector inductively coupled plasma mass spectrometry. *Journal of Analytical Atomic Spectrometry* **2006**, *21* (4), 427-430.
(45) Zhu, Z.; Meija, J.; Zheng, A.; Mester, Z.; Yang, L. Determination of the isotopic composition of iridium using multicollector-ICPMS. *Analytical Chemistry* **2017**, *89* (17), 9375-9382.
(46) Yang, L.; Tong, S.; Zhou, L.; Hu, Z.; Mester, Z.; Meija, J. A critical review on isotopic fractionation correction methods for accurate isotope amount ratio measurements by MC-ICP-MS. *Journal of Analytical Atomic Spectrometry* **2018**, *33* (11), 1849-1861.
(47) Costas-Rodríguez, M.; Anoshkina, Y.; Lauwens, S.; Van Vlierberghe, H.; Delanghe, J.; Vanhaecke, F. Isotopic analysis of Cu in blood serum by multi-collector ICP-mass spectrometry: a new approach for the diagnosis and prognosis of liver cirrhosis? *Metallomics* **2015**, *7* (3), 491-498.
(48) Costas-Rodríguez, M.; Van Campenhout, S.; Hastuti, A. A.; Devisscher, L.; Van Vlierberghe, H.; Vanhaecke, F. Body distribution of stable copper isotopes during the progression of cholestatic liver disease induced by common bile duct ligation in mice. *Metallomics* **2019**, *11* (6), 1093-1103.
(49) Dauphas, N.; Schauble, E. A. Mass fractionation laws, mass-independent effects, and isotopic anomalies. *Annual Review of Earth and Planetary Sciences* **2016**, *44*, 709-783.
(50) Bolea-Fernandez, E.; Balcaen, L.; Resano, M.; Vanhaecke, F. Potential of methyl fluoride as a universal reaction gas to overcome spectral interference in the determination of ultratrace concentrations of metals in biofluids using inductively coupled plasma-tandem mass spectrometry. *Analytical chemistry* **2014**, *86* (15), 7969-7977.